Developmental Cell
Article

Cell PRESS

An HMGA2-IGF2BP2 Axis Regulates Myoblast Proliferation and Myogenesis

Zhizhong Li,[1] Jason A. Gilbert,[1] Yunyu Zhang,[1] Minsi Zhang,[2] Qiong Qiu,[3] Krishnan Ramanujan,[1] Tea Shavlakadze,[1] John K. Eash,[1] Annarita Scaramozza,[4] Matthew M. Goddeeris,[5] David G. Kirsch,[2,3] Kevin P. Campbell,[5] Andrew S. Brack,[4] and David J. Glass[1,*]

[1]Novartis Institutes for Biomedical Research, Cambridge, MA 02139, USA
[2]Department of Pharmacology and Cancer Biology
[3]Department of Radiation Oncology
Duke University Medical Center, Durham, NC 27710, USA
[4]Center of Regenerative Medicine, Massachusetts General Hospital and Harvard Stem Cell Institute, Harvard University, Boston, MA 02114, USA
[5]Howard Hughes Medical Institute, Senator Paul D. Wellstone Muscular Dystrophy Cooperative Research Center Department of Molecular Physiology and Biophysics, Department of Neurology, and Department of Internal Medicine, Roy J. and Lucille A. Carver College of Medicine, The University of Iowa, Iowa City, IA 52242, USA
*Correspondence: david.glass@novartis.com
http://dx.doi.org/10.1016/j.devcel.2012.10.019

SUMMARY

A group of genes that are highly and specifically expressed in proliferating skeletal myoblasts during myogenesis was identified. Expression of one of these genes, *Hmga2*, increases coincident with satellite cell activation, and later its expression significantly declines correlating with fusion of myoblasts into myotubes. *Hmga2* knockout mice exhibit impaired muscle development and reduced myoblast proliferation, while overexpression of HMGA2 promotes myoblast growth. This perturbation in proliferation can be explained by the finding that HMGA2 directly regulates the RNA-binding protein IGF2BP2. Add-back of IGF2BP2 rescues the phenotype. IGF2BP2 in turn binds to and controls the translation of a set of mRNAs, including *c-myc*, *Sp1*, and *Igf1r*. These data demonstrate that the HMGA2-IGF2BP2 axis functions as a key regulator of satellite cell activation and therefore skeletal muscle development.

INTRODUCTION

Myogenesis, which occurs during both postnatal growth and the regeneration of skeletal muscle after an injury, is a highly ordered process that can be subdivided into multiple steps. These steps include the activation of muscle stem cells, differentiation of these stem cells into committed myoblasts, followed by proliferation and then differentiation of myoblasts, resulting in cell fusion—to form multinucleated myotubes (Le Grand and Rudnicki, 2007). Sequential activation of the muscle-specific transcriptional factors including Pax3, Pax7, Myf5, MyoD, Myogenin, and Myf6 plays a crucial role in regulating myogenesis (Le Grand and Rudnicki, 2007). However, the precise mechanism controlling temporal regulation of myogenesis remains largely unknown.

HMGA2 is a transcriptional coregulator belonging to a family of small high-mobility-group (HMG) proteins containing AT-hook DNA binding domains. HMGA proteins may modulate gene expression by altering chromatin architecture and/or by recruiting other proteins to the transcription regulatory complex (Pfannkuche et al., 2009). HMGA2 is highly expressed in various undifferentiated tissues during embryonic development but is turned off in most adult tissues (Ashar et al., 2010; Pfannkuche et al., 2009). Furthermore, HMGA2 is frequently found to be upregulated in tumor samples, implying that it may play a role in controlling cell proliferation (Fedele and Fusco, 2010; Li et al., 2011; Watanabe et al., 2009).

Recent studies have suggested that HMGA2 is expressed and may play a role in maintaining certain adult stem/progenitor cells, including, for example, the maintenance of neural stem/progenitor cells (Nishino et al., 2008). It has recently been reported that HMGA2 is indispensable for the self-renewal of young but not old neural stem cells, partially through regulating p16[Ink4A] (Nishino et al., 2008). However, the regulation of HMGA2 on p16 [Ink4A] appears to be indirect, and other critical downstream effectors of HMGA2 remain to be determined. Studies of HMGA2 in myogenesis have been inconclusive. Previous work in tissue culture systems suggested that overexpression of HMGA2 in embryonic stem (ES) cells could enhance myogenesis and myosin heavy chain (MHC) expression (Caron et al., 2005). But it is unclear whether HMGA2 does so simply by promoting the differentiation of ES cells toward a myogenic lineage or whether HMGA2 directly promotes the terminal differentiation of myoblasts.

IGF2BP2 is a member of the IGF2 mRNA-binding protein (IMP) family, which includes IGF2BP1-3. IGF2BP2 contains four KH domains and two RRM domains and can bind to various RNAs (Christiansen et al., 2009). IGF2BP2 was shown to bind to *Igf2* mRNA and enhances IGF2 translation (Dai et al., 2011). Whether IGF2BP2 also regulates the translation of other mRNAs is unknown. HMGA2 could regulate the transcription of *Igf2bp2* during embryonic development (Cleynen et al., 2007), but the biological significance of this regulation was unknown. Similar to *Hmga2*, *Igfbps* are "oncofetal" genes that are highly

expressed during embryonic development, usually downregulated in adult tissues and reactivated in various cancers. *Igf2bp2* is best known for its genetic variance linked to the risk of type 2 diabetes (Christiansen et al., 2009). However, few functional studies of IGF2BP2 have been reported, and a potential role in controlling cell proliferation or myogenesis has not been previously addressed.

In the current study, we sought to identify critical factors regulating muscle stem cell activation and commitment, and determined through both gain-of-function and loss-of-function analyses that HMGA2 is a key regulator of myogenesis, both in vitro and in vivo, acting via IGF2BP2.

RESULTS

Identification of Genes that Are Markers for Proliferating Muscle Progenitors during Myogenesis

Activation of quiescent satellite cells, as measured by their stimulation to proliferate, is a critical early event in regeneration (Le Grand and Rudnicki, 2007). We asked whether genes that are specifically expressed in proliferating myoblasts have a required role in myogenesis. Genes that were expressed in proliferating myoblasts but not in satellite cells were determined by analyzing microarray data from both published data (Fukada et al., 2007) and an internal expression study (Figure S1A available online). A total of 642 individual genes whose mRNA levels are at least 5-fold higher in proliferating myoblasts in comparison to quiescent satellite cells were labeled as constituting a "Proliferation Signature" (Figure S1A). Next, microarray data from a myoblast differentiation time course experiment allowed for the identification of a group of 328 genes as a "Differentiation Signature"—these were genes whose levels decrease during muscle differentiation, dropping by more than 80% at day 5 in comparison to day 0 of differentiation (Figure S1A). By overlapping the two gene sets, 139 genes were left that are expressed at high levels in proliferating myoblasts but that are not expressed to an appreciable degree in satellite cells or in day 5 differentiated myotubes (Figure S1A; Table S1). This last group of genes constitutes a "Myoblast Signature." Consistent with their association with proliferative status, genes in the Myoblast Signature are highly enriched for cell cycle regulators such as *Cyclin B1*, *Cyclin A2*, and *Cdc2a* (Table S1). There is also a large group of genes that are involved in modulating cell checkpoints and maintaining genome stability during mitosis, such as *Cenpa*, *Brca1*, *Aurka*, *Aurkb*, *Mcm5*, and *Rad51* (Table S1). However, many genes in the Myoblast Signature do not have well-documented roles in muscle development, and therefore require further study. Of those, *Hmga2* was particularly striking in that its mRNA level increased most after satellite cell activation (more than 30-fold) and rapidly turned off during terminal differentiation.

Hmga2 Is Increased upon Proliferation of Mouse Myoblasts but Rapidly Downregulated upon Differentiation

To determine the reproducibility of the *Hmga2* mRNA pattern obtained from the microarray data, quantitative RT-PCR (qRT-PCR) for *Hmga2* was performed on freshly isolated satellite cells obtained from the C57BL/6 mouse, which were then induced to

become proliferating myoblasts and subsequently differentiated into myotubes (Figures S1B and S1C). qRT-PCR further confirmed that cells demonstrated gene perturbations consistent with their activation and proliferation, such as regulation of *Pax7*, *MyoD*, and *Myf5* (Figure S2A).

We then sought to use qRT-PCR to verify the microarray-obtained pattern of *Hmga2* expression during myogenesis. By qRT-PCR, *Hmga2* mRNA levels were found to strongly increase when satellite cells were activated to proliferate, becoming committed myoblasts (Figure 1A). When myoblasts were induced to differentiate, the *Hmga2* mRNA level then gradually decreased (Figure 1A). These data demonstrated that *Hmga2* mRNA was positively associated with proliferative activity of myogenic cells, and negatively correlated with terminal differentiation.

The HMGA2 protein level was next determined. Consistent with the high mRNA level, immunofluorescence demonstrated that HMGA2 protein was easily visible in myoblasts, and exclusively localized to the nuclei, consistent with its role as a DNA binding protein (Figure S2B). When the mouse myoblasts were switched to differentiation medium, HMGA2 protein level continuously decreased (Figure 1B). This same pattern of HMGA2 protein was also observed in C2C12 cells, a commonly used immortalized mouse myoblast cell line (Figure S2C).

In order to further investigate the relationship between HMGA2 protein expression and myoblast differentiation at the single cell level, immunofluorescence of HMGA2 and MHC was performed on partially differentiated primary myoblasts. While 35%-45% of the nuclei of total cultured cells stained positive for HMGA2, essentially all MHC positive (MHC+) terminal-differentiated myotubes were HMGA2 negative (HMGA2−) (Figure 1C). Therefore, HMGA2 and MHC expression are mutually exclusive.

Thus, *Hmga2* mRNA and protein levels are upregulated in proliferating myoblasts and subsequently become downregulated coincident with differentiation.

HMGA2 Is Expressed in Neonatal and Regenerating Muscle but Not in Mature Muscle In Vivo

After observing that HMGA2 is specifically expressed in cultured proliferating myoblasts in vitro, it was of interest to analyze the relative levels of HMGA2 protein in skeletal muscle cells in vivo. Neonatal muscle and regenerating muscle were examined, because these two sources contain proliferating muscle progenitor cells (myoblasts). Adult skeletal muscle, which has very low myogenic activity and therefore lacks appreciable numbers of activated myoblasts, was also analyzed as a control.

By western blot, HMGA2 protein was detected in neonatal but not adult skeletal muscles (Figure 1D). Double immunofluorescence of HMGA2/ Pax7, or HMGA2/MyoD further revealed that HMGA2 protein expression was coincident with Pax7 or MyoD (Figure 1E), demonstrating that HMGA2 is highly expressed in proliferating myoblasts in vivo.

Induction of regeneration in adult skeletal muscle, using cardiotoxin (CTX), also makes it possible to identify populations of proliferating and differentiating myoblasts. A time-course of muscle regeneration was analyzed using H&E-stained sections from muscles sampled 3, 7, and 14 days following CTX administration (Figure S2D). As expected in this model, there was an initial inflammatory cell infiltration at day 3 following injury. Newly
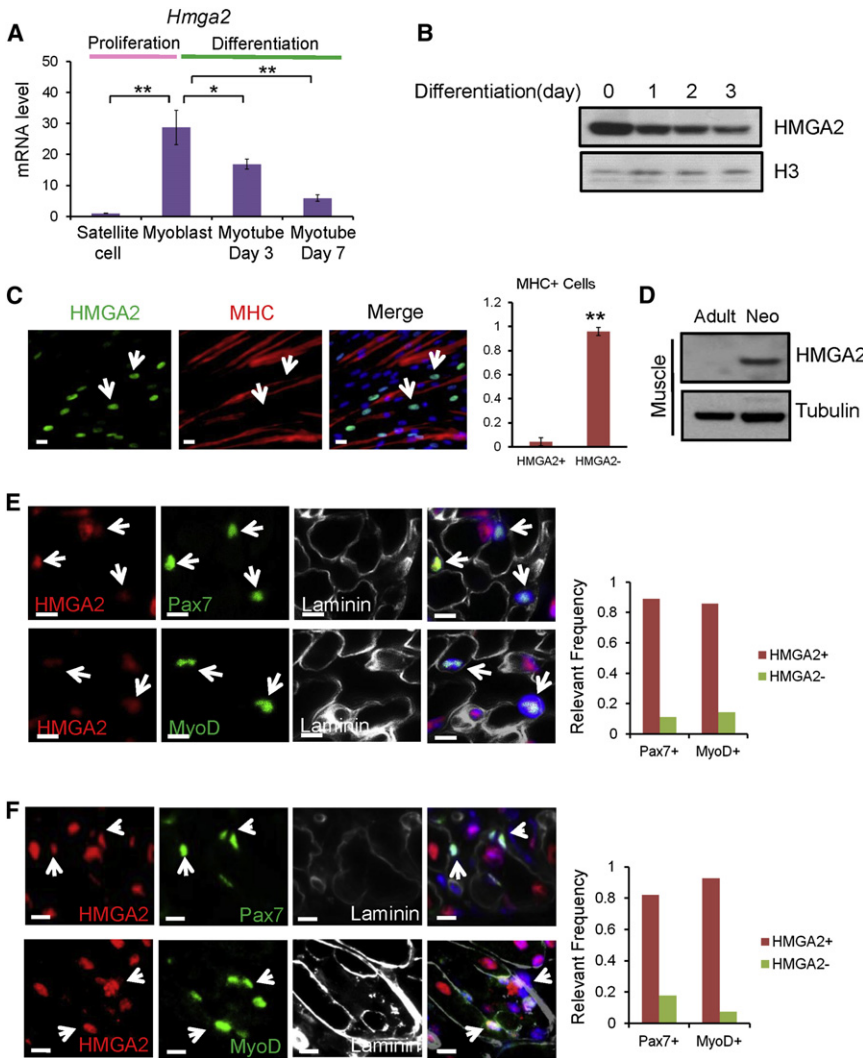
Figure 1. Hmga2 Is a Signature Gene in Undifferentiated Myoblasts In Vitro and In Vivo

(A) Real-time PCR verified that *Hmga2* mRNA is upregulated upon satellite cell activation, remains upregulated during the proliferation phase, and turns off during myoblast differentiation. Fresh satellite cells were isolated from 8-week-old C57BL/6 mice, as reported before. Cells were directly sorted into TRIzol for mRNA isolation (satellite cells) or cultured in proliferation medium for 4 days (myoblasts) and then switched to differentiation medium (myotube day 3 and day 7) for another 7 days. Real-time PCR was performed to quantify *Hmga2* mRNA level. Data were normalized to *Gapdh* and *18 s* mRNAs. *Hmga2* mRNA in quiescent satellite cell was set as 1.0. Error bars depict mean ± SEM.

(B) HMGA2 protein levels gradually decreased during primary myoblast differentiation. Primary myoblasts were cultured in growth medium to reach 80% confluence and switched into differentiation medium for up to 3 days. Nuclei proteins were isolated and western blots were performed using antibodies against HMGA2 and Histone H3.

(C) HMGA2 expression is inversely correlated with terminal muscle differentiation. Primary myoblasts were grown to >80% confluence in proliferation medium and switched to differentiation medium for 2 days. Cells were then fixed and stained for HMGA2 and MHC. At this stage, 30%~40% cells became terminally differentiated, as evidenced by MHC expression (scale bar: 50 μm). Most MHC positive cells are negative for HMGA2 (white arrow: HMGA2+ MHC− nuclei). More than 95% of nuclei of MHC positive cells are HMGA2 negative. MHC+ nuclei represent nuclei that are associated with cytoplasmic MHC expression. **p < 0.01 versus HMGA2+ nuclei in MHC+ subset. Error bars depict mean ± SEM.

(D) Muscle protein samples were harvested from postnatal (1 day) or adult (12 weeks) C57BL/6 mice and western blots were performed, using antibodies against HMGA2 and α-tubulin. HMGA2 protein is detected in neonatal but not adult skeletal muscle tissues. Neo, neonatal.

(E) Immunofluorescence demonstrates that HMGA2 is colocalized with Pax7 and MyoD in the nuclei of neonatal muscle tissues. Neonatal muscle was stained using antibodies against HMGA2, or Pax7, or Laminin or MyoD. DAPI was used to stain nuclei. White arrow indicates Pax7/HMGA2 double-positive or MyoD/HMGA2 double-positive cells (scale bar: 10 μm) Quantification of staining demonstrates that more than 80% Pax7+ or MyoD+ myoblasts are also HMGA2+.

(F) Immunofluorescence demonstrates that HMGA2 is colocalized with Pax7 and MyoD in the nuclei of regenerating muscle tissues. Mouse TA muscle was treated with dry ice to induce a muscle injury, as previously reported (see Experimental Procedures), and muscle samples were harvested 5 days later. Muscle samples were stained using antibodies against HMGA2, or Pax7, or Laminin or MyoD. DAPI was used to stain nuclei. White arrow indicates Pax7/HMGA2 double-positive or MyoD/HMGA2 double-positive cells (scale bar: 10 μm) Quantification of staining demonstrates that more than 80% Pax7+ or MyoD+ myoblasts are also HMGA2+.

See also Figure S2 and Table S1.

formed immature myotubes with centralized nuclei were widely observable at day 7, and the area of injury was fully regenerated at day 14. After performing HMGA2 and Desmin double-immunofluorescence staining, HMGA2 was not detected in uninjured adult muscle. However, at day 3 following injury, many mononucleated cells present in the injury site stained intensely for HMGA2. At day 7, HMGA2 was mainly detected in the centralized nuclei located within newly formed myofibers. At day 14, HMGA2 protein level further decreased but was still present in nuclei of some regenerated myofibers (Figure S2D). Therefore,

HMGA2 is only expressed in immature myogenic cells, including myoblasts, during regeneration.

To test whether HMGA2 is reproducibly induced during regeneration, as opposed to being idiosyncratically induced by cardiotoxin, a second, well-established model of muscle injury was analyzed: freezing the muscle to cause an injury and thereby induce regeneration. HMGA2 was found to be strongly induced 5 days after freezing injury (Figure 1F), detectable in centralized nuclei. Interestingly, more than 80% of Pax7+ or MyoD+ cells also expressed HMGA2 (Figure 1F), further demonstrating that
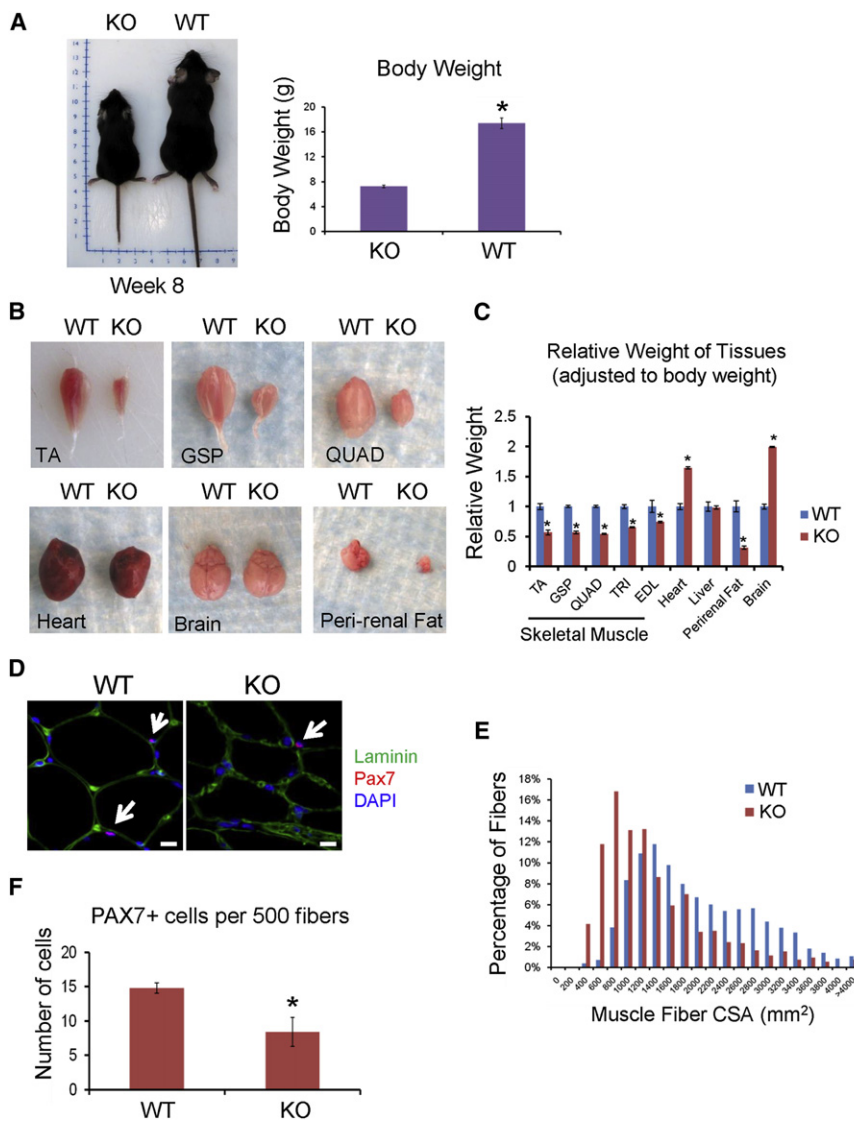
Figure 2. Hmga2 Knockout Mice Demonstrate Deficiency in Muscle Growth

(A) Comparison of female *Hmga2* knockout (KO) and wild-type (WT) mice at 8 weeks of age. As reported previously, the *Hmga2* KO mice have a "pygmy" phenotype, with a body weight of about 40% of WT littermates. *$p < 0.05$ Hmga2 KO mice versus WT mice. Error bars depict mean ± SEM.

(B) Side-by-side comparison of various tissues including skeletal muscle from *Hmga2* KO and WT mice. TA, tibialis anterior; GSP, soleus-gastrocnemius-plantaris complex; QUAD, quadricep. All organs examined were smaller in *Hmga2* KO mice.

(C) The weights of various tissues were normalized to body weight. After normalization, all examined skeletal muscle tissues from *Hmga2* KO mice were still significantly smaller than those from *Hmga2* WT mice. In contrast, the brain and heart were proportionally larger in *Hmga2* KO mice, while the relative weight of liver was almost identical in both genotypes. Consistent with a previous report, *Hmga2* KO mice showed depletion of fat tissue, represented by perirenal fat. *$p < 0.05$ *Hmga2* KO mice versus WT mice. Error bars depict mean ± SEM.

(D) Immunofluorescence of Pax7, Laminin, and DAPI on cross-sections of *Hmga2* KO and WT mice. *Hmga2* KO mice show a smaller cross-section area (CSA) and reduced Pax7 staining. Arrows indicate Pax7+ cells. Scale bar represents 50 μm.

(E) Comparison of CSA from *Hmga2* WT and KO mice reveal that *Hmga2* KO mice have smaller myofibers. Histogram demonstrates an enrichment of small muscle fibers and lack of big fibers in *Hmga2* KO mice versus *Hmga2* WT mice.

(F) *Hmga2* KO mice had fewer Pax7+ cells per 500 fibers. At least 3,000 fibers were counted for each sample. *$p < 0.05$ *Hmga2* KO mice versus *Hmga2* WT mice. Error bars depict mean ± SEM.

See also Figure S3.

HMGA2 is expressed in immature muscle cells during early myogenesis in vivo.

Skeletal Muscle Is Severely Compromised in Adult Hmga2 Knockout Mice

Next *Hmga2* knockout (KO) mice were studied to determine HMGA2's in vivo requirement. Mice that are null for *Hmga2* had been reported to demonstrate a decrease in fat tissue (Anand and Chada, 2000), but their skeletal muscle had not been characterized before. As shown previously, adult *Hmga2* KO mice have a pygmy phenotype and are significantly smaller than wild-type (WT) littermates. Their body weight was only about 40% of that of WT littermates at 8 weeks of age (Figure 2A). Comparison of KO hindlimb muscles to those from WT animals revealed a significant decrease in relative skeletal muscle size in *Hmga2* KO mice (Figures 2B and S3A); because *Hmga2* KO mice were significantly smaller than WT littermates, we normalized all the organ weights to the body weight. Interestingly, the normalized weights of these organs demonstrated that only the

skeletal muscle and fat tissues were smaller out-of-proportion to the body weight (Figure 2C). For example, after body weight normalization, liver weight was almost identical between *Hmga2* KO and WT mice, and the heart and brain were actually proportionally larger in *Hmga2* KOs (Figure 2C) These data suggest that HMGA2 is particularly important for skeletal muscle growth.

To understand the nature of the hypotrophic skeletal muscle observed in *Hmga2* KO mice, skeletal muscle cross-sections from *Hmga2* KO and WT mice were stained by hematoxylin and eosin (H&E) or immunostained with an anti-Laminin antibody (Figures 2D and S3B); the *Hmga2* KO mice had a prevalence of smaller myofibers, demonstrated by a reduced cross-section area (CSA), in comparison to WT littermates (Figures 2E, S3B, and S3C). Because HMGA2 is mostly expressed in undifferentiated myoblasts, the muscle stem/progenitor cell number was counted in *Hmga2* KO and WT mice by Pax7 staining. There was a significant, 40%~50%, decrease of Pax7+ cell number in *Hmga2* KO mice (Figure 2F), suggesting that the lack of
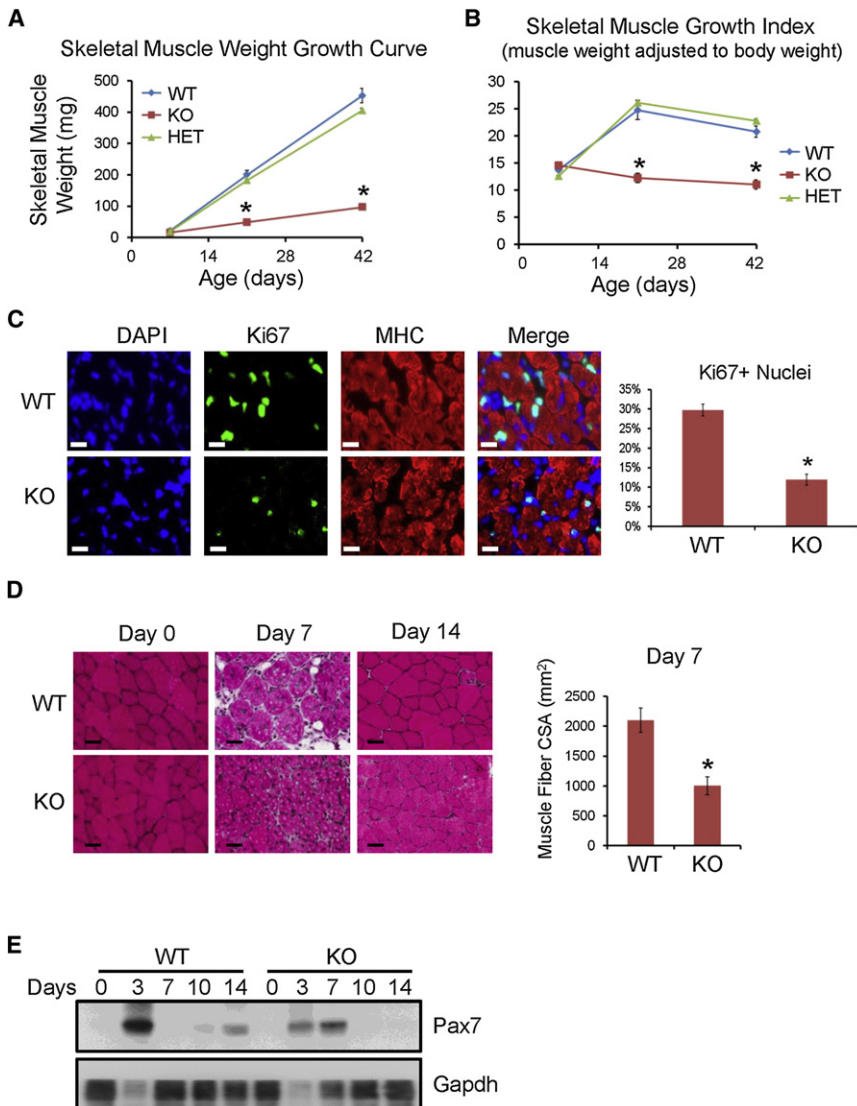
Figure 3. Hmga2 KO Mice Have Significant Deficiency in Muscle Growth during the Postnatal Growth Phase

(A) Postnatal skeletal muscle growth is severely impaired in *Hmga2* KO mice. *Hmga2* WT and KO mice were sacrificed at day 7, day 21, and day 42 after birth, and skeletal muscle from hindlimbs were collected and weighed Skeletal muscle growth in *Hmga2* KO was significantly slower than those in WT or Het littermates. *$p < 0.05$ *Hmga2* KO mice versus *Hmga2* WT mice. Error bars depict mean ± SEM.

(B) Early skeletal muscle growth is most affected by the loss of *Hmga2*. Data from (A) were normalized to mouse body weight at different time points. While both WT and Het mice showed strong muscle growth between day 7 and day 21, this growth phase was essentially abolished in *Hmga2* KO mice. *$p < 0.05$ *Hmga2* KO mice versus *Hmga2* WT mice. Error bars depict mean ± SEM.

(C) *Hmga2* KO mice show decreased cell proliferation during neonatal growth phase. TA muscle from 7-day-old *Hmga2* WT and KO mice were harvested, fixed, and stained for antibodies as indicated. *Hmga2* KOs showed significant reduction of Ki67+ nuclei in skeletal muscle samples, indicating impaired cell proliferation in vivo. *$p < 0.05$ versus *Hmga2* WT mice sample. Error bars depict mean ± SEM.

(D) *Hmga2* KO mice form smaller fibers during regeneration. *Hmga2* KO and WT mice were injected with 10 μM CTX and samples were harvested 7 days and 14 days after injection. H&E staining was performed. Both KO and WT muscles fully regenerated at day 14. Newly formed myofibers, judged by their centralized nuclei, were significantly smaller in *Hmga2* KO mice. *$p < 0.05$ versus *Hmga2* WT sample. Error bars depict mean ± SEM.

(E) *Hmga2* KO mice have weakened and delayed regeneration. *Hmga2* KO and WT mice were injected with 10 μM CTX and protein samples were harvested 3, 7, 10, and 14 days after injury. Pax7 western blots indicated that Pax7 level is higher in WT muscle at day 3. Pax7 protein is persistent in KO but not WT samples at day 7.

See also Figure S4.

HMGA2 causes a decreased muscle progenitor pool—leading to smaller muscle fibers.

Because the skeletal muscle phenotype had not been studied in *Hmga2* KO mice before, we decided to further characterize these mice, by initially tracking body and muscle weights after birth. At day 7, *Hmga2* KO mice were only slightly smaller than WT mice (Figure S4A). However, the growth of *Hmga2* KO mice was significantly impaired during the postnatal growth phase, particularly between day 14 and 28 (Figure S4A). In addition to body weight, skeletal muscle weights were only modestly lower at day 7, but then were increasingly retarded in growth between day 7 and 42 (Figure 3A). The skeletal muscle growth index, a number generated by normalizing skeletal muscle weight to whole animal body weight, was calculated at days 7, 21, and 42 (Figure 3B). In contrast to the WT animals, which demonstrated the expected increase in muscle growth, *Hmga2* KO mice experienced an almost flat skeletal muscle growth

index throughout the growth period (Figure 3B). The significant deficiency in skeletal muscle growth between day 7 and 21 in KOs suggests that HMGA2 is particularly crucial for early postnatal skeletal muscle growth, consistent with a role in muscle satellite cell activation and proliferation.

To directly examine cell proliferation, immunofluorescence of cell proliferation marker Ki67 on neonatal muscle samples from *Hmga2* KO and WT mice was performed. Samples from *Hmga2* KO mice demonstrated a significant, 50%∼60%, reduction in the number of Ki67+ cells in comparison to WT control (Figure 3C). No significant apoptosis signal was detected in either *Hmga2* KO or WT samples by cleaved PARP antibody or TUNEL assays in vivo (data not shown). These data indicate that reduced cell proliferation in *Hmga2* KO mice could contribute to the defect in muscle growth.

Reduced myoblast proliferation may have consequence not only on neonatal muscle growth but also muscle regeneration;
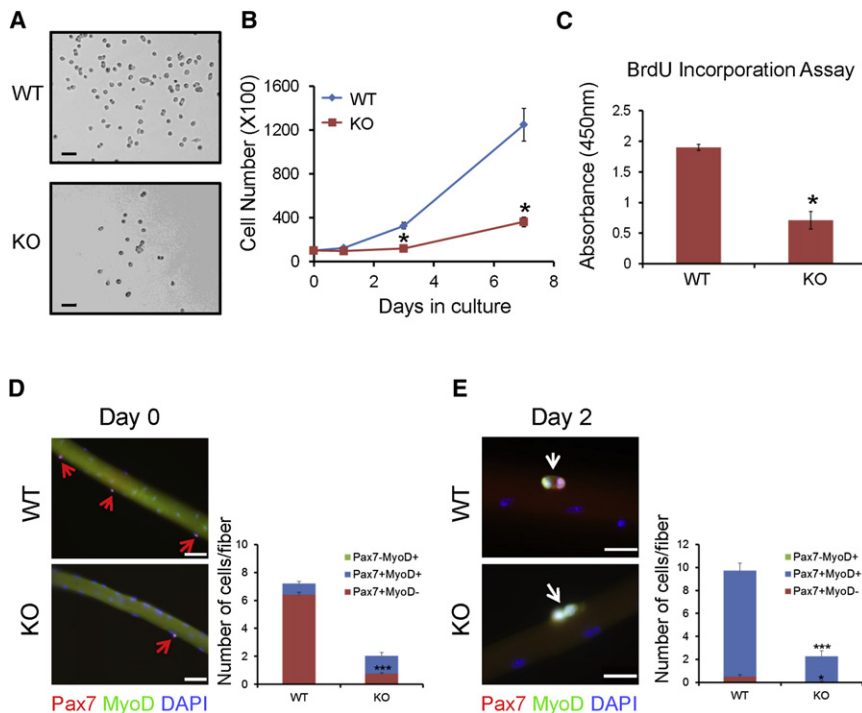
Figure 4. Hmga2 KO Myoblasts Demonstrated Reduced Cell Proliferation and Self-Renewal

(A) Myoblasts from *Hmga2* KO mice show decreased cell proliferation. Myoblasts were isolated from *Hmga2* WT and KO mice. A total of 2,000 myoblasts were seeded into each well of 96-well plates. Pictures were taken 7 days after seeding.

(B) Myoblasts from *Hmga2* KO mice grow slower than those from WT. Myoblasts were isolated from *Hmga2* WT and KO mice. A total of 10,000 myoblasts were seeded into each well of 24-well plates. Cell numbers were counted at day 1, day 3, and day 7 after seeding. *p < 0.05 versus Hmga2 WT sample at the same time point. Error bars depict mean ± SEM.

(C) *Hmga2* KO myoblasts have decreased BrdU incorporation in proliferation medium. A total of 5,000 myoblasts from *Hmga2* KO and WT mice were seeded into each well of 96-well plates. BrdU assays were performed by BrdU Cell Proliferation Assay Kit (Cell Signaling Technology) according to the manufacturer's guidance. *p < 0.05 versus *Hmga2* WT sample. Error bars depict mean ± SEM.

(D) *Hmga2* KO myofibers are smaller and contain fewer satellite cells. Fresh isolated single fibers from WT and KO mice were fixed and stained for Pax7 to label satellite cells. ***p < 0.01 versus *Hmga2* WT sample. Error bars depict mean ± SEM.

(E) Hmga KO fibers have decreased number of asymmetric satellite cell divisions. *Hmga2* KO and WT myofibers were cultured for 2 days to allow satellite cell activation. Fibers were fixed and stained for Pax7 and MyoD. A small percentage of WT satellite cells was dividing asymmetrically. No asymmetric divisions were observed in *Hmga2* KO myofibers. ***p < 0.01, *p < 0.05 versus *Hmga2* WT sample. Error bars depict mean ± SEM.
See also Figure S5.

we therefore compared *Hmga2* KO and WT mice after CTX induced muscle regeneration. At day 7 and day 14 after injury, the regenerating fibers were much smaller in *Hmga2* KO mice, with an average 50% reduction in CSA (Figure 3D). Other than that, *Hmga2* WT and KO samples showed similar morphology in general, such as the presence of centralized nuclei and a similar degree of inflammation at day 7, and almost complete regeneration at day 14 (Figure 3D). To further compare the differences of WT and *Hmga2* KO muscles during regeneration, protein samples were harvested and western blots were performed. In comparison to WT, KO muscle samples showed much weaker Pax7 activation at day 3, consistent with fewer satellite cells/muscle fibers in KO mice. Interestingly, at day 7, while Pax7 levels had significantly decreased in WT muscle, Pax7 levels remained high in KO muscles. Therefore, regeneration can be completed in *Hmga2* KO muscle, but the process was delayed and resulted in smaller muscles.

Muscle atrophy in WT myofibers can be induced by a variety of cachectic stimuli, resulting in part from protein degradation caused by induction of the E3 ubiquitin ligases MuRF1 and MAFbx (Bodine et al., 2001). To determine whether the decrease in muscle mass caused by *Hmga2* loss could be partially due to an induction in muscle atrophy pathways, mRNA levels of *MuRF1* and *MAFbx* were determined; neither were significantly changed (Figure S4B), demonstrating that HMGA2 does not affect these atrophy pathways.

HMGA2 Affects Myoblast Proliferation and Cell Fate Decision

To directly examine whether *Hmga2* KO has a defect in myoblast proliferation, we next compared the growth rate of myoblasts isolated from *Hmga2* KO and WT mice. Myoblasts were successfully cultured for more than 20 passages. *Hmga2* KO myoblasts demonstrated slower growth rates (Figures 4A and 4B) and lower BrdU incorporation than WT controls (Figure 4C). To investigate whether HMGA2 also regulates differentiation, myoblasts were grown and differentiated in vitro. Because myoblast differentiation could be affected by cell density, we performed differentiation experiments under both low and high cell density. When cells were seeded at low density and allowed to proliferate for 2 days before serum was withdrawn, the number of myotubes formed with multiple nuclei was significantly reduced in cells obtained from the *Hmga2* KO mice (Figure S5A). However, when myoblasts were seeded at high density and induced to differentiate without proliferation, no difference was observed. Both WT and KO myoblasts differentiated well and were stained strongly by MHC (Figure S5B). Therefore, HMGA2 is not required for myoblast terminal differentiation, but it does perturb proliferation, and thus differentiation is affected when cell numbers are limiting.

Genes regulating myoblast proliferation may also play roles in cell fate decisions. To examine whether HMGA2 has a role in this process, we isolated single fibers from both *Hmga2* WT and KO muscles. Consistent with previous findings, KO fibers were
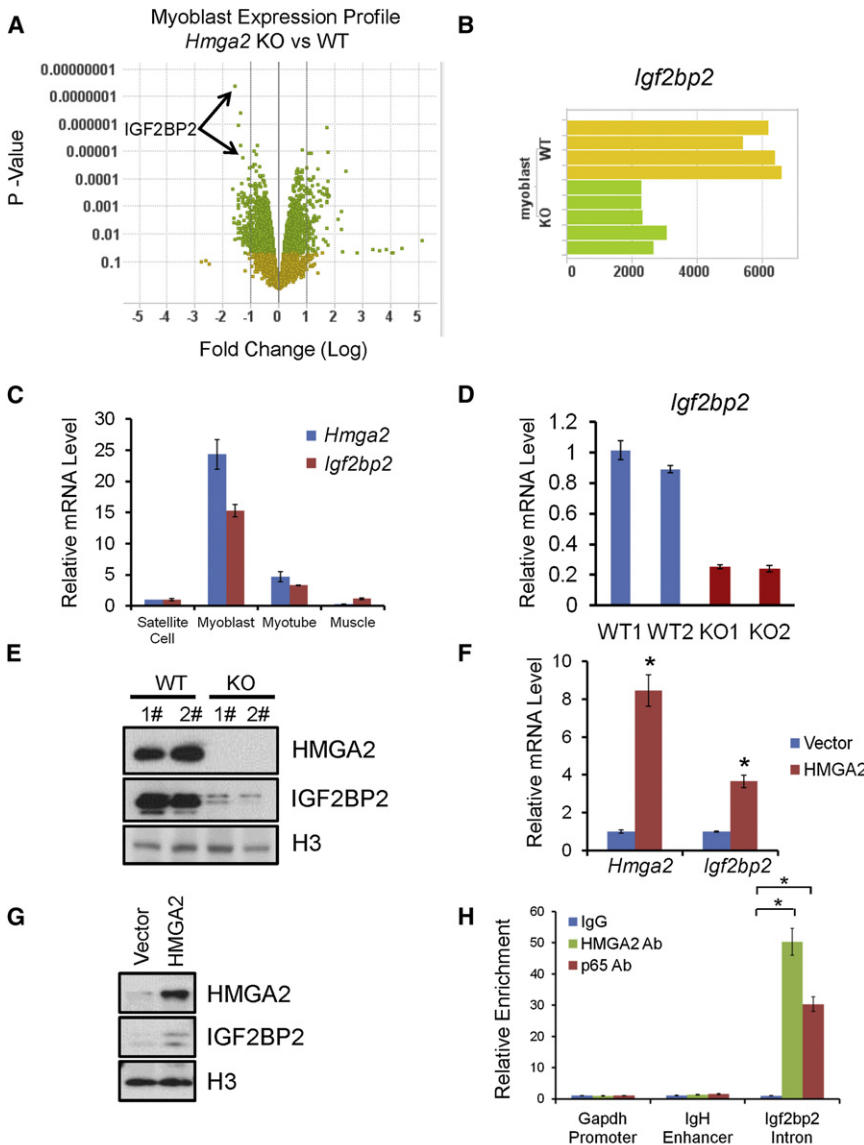
Figure 5. HMGA2 Regulates IGF2BP2 in Myoblasts

(A) *Igf2bp2* is one of the top genes regulated by HMGA2 in myoblasts. "Volcano Plot" of microarray data showing expression profiles of *Hmga2* KO and WT myoblasts. *Igf2bp2* is one of the most significantly downregulated genes in *Hmga2* KO myoblasts.

(B) Microarray data show that *Igf2bp2* is downregulated in *Hmga2* KO myoblasts. Myoblasts isolated from four WT and five KO mice were used for microarray analysis.

(C) *Hmga2* and *Igf2bp2* have similar expression patterns during myogenesis. mRNAs were harvested from freshly isolated satellite cells, myoblasts, immature myotubes (day 3 differentiation), and mature muscle samples. RT-PCR assays were performed to examine the expression of *Hmga2* and *Igf2bp2* mRNA levels. Data were normalized to *Gapdh* and *18 s* mRNAs. Error bars depict mean ± SEM.

(D) *Igf2bp2* mRNA is downregulated in *Hmga2* KO myoblasts. mRNA samples were harvested from two *Hmga2* KO and two *Hmga2* WT myoblasts. RT-PCRs were performed to examine *Igf2bp2* level. Data were normalized to *Gapdh* and *18 s* mRNAs. Error bars depict mean ± SEM.

(E) IGF2BP2 protein is downregulated in *Hmga2* KO myoblasts. Protein samples were harvested from two *Hmga2* KO and two plates of *Hmga2* WT myoblasts. Western blots were performed using antibodies against HMGA2, IGF2BP2, and Histone H3.

(F) Overexpression of HMGA2 in myoblasts increases *Igf2bp2* mRNA levels. Lentiviral constructs expressing HMGA2 or empty control were used to infect myoblasts, and 72 hr after infection, mRNAs were harvested and RT-PCRs were performed to examine mRNA levels of *Hmga2* and *Igf2bp2*. Data were normalized to *Gapdh* and *18 s* mRNAs. *p < 0.05 HMGA2 overexpression versus vector control sample. Error bars depict mean ± SEM.

(G) Exogenous expression of HMGA2 in myoblasts increases IGF2BP2 protein. Lentiviral constructs expressing HMGA2 or empty control were used to infect myoblasts. 72 hr after infection, protein samples were harvested and western blots were performed using antibodies against HMGA2, IGF2BP2, and Histone H3.

(H) HMGA2 protein directly binds to *Igf2bp2* first intron region. Myoblast cells were fixed and chromatin IP was performed using IgG or antibodies against HMGA2 or p65. After DNA elution, primers sets detecting *Gapdh* promoter, *IgH* enhancer, and *Igf2bp2* first intron sequences were used for RT-PCR analysis. HMGA2 and p65 showed enriched binding to *Igf2bp2* intron, but they were not recruited to *Gapdh* promoter or *IgH* enhancer. *p < 0.05 with comparison of relative recruitment of HMGA2 or p65 and IgG to *Igf2bp2* Intron region. Error bars depict mean ± SEM.

See also Table S2.

smaller in diameter and have significantly fewer satellite cells per fiber (Figure 4D). After 2 days in culture, when satellite cells undergo their first division (Rudnicki et al., 2008; Zammit et al., 2004), most satellite cells from WT muscle appeared as doublets, both expressing Pax7+/MyoD+, consistent with symmetric divisions. A small percentage of satellite cells divide asymmetrically, with one cell retaining MyoD and the other losing MyoD, indicating that a fraction of satellite cells reacquire a self-renewing fate (Olguin and Olwin, 2004; Zammit et al., 2004). By contrast, all *Hmga2* KO satellite cells were MyoD+ and therefore had divided symmetrically (Figure 4E). In conclusion, losing HMGA2 not only decreased myoblast growth, but

also reduced the self-renewal potential of satellite cells. These data help explain the reduced number of satellite cells and smaller fibers observed in *Hmga2* KO mice.

IGF2BP2 Is a Top HMGA2 Target in Myoblasts

It was next important to investigate the mechanism by which HMGA2 controls myoblast proliferation and early myogenesis. mRNAs were isolated from *Hmga2* KO and WT myoblasts, and a microarray was performed. A total of 28 genes were found to be significantly downregulated and 30 genes were significantly upregulated in *Hmga2* KO myoblasts in comparison to WT samples (fold change > 2, p < 0.001) (Figure 5A; Table S2).
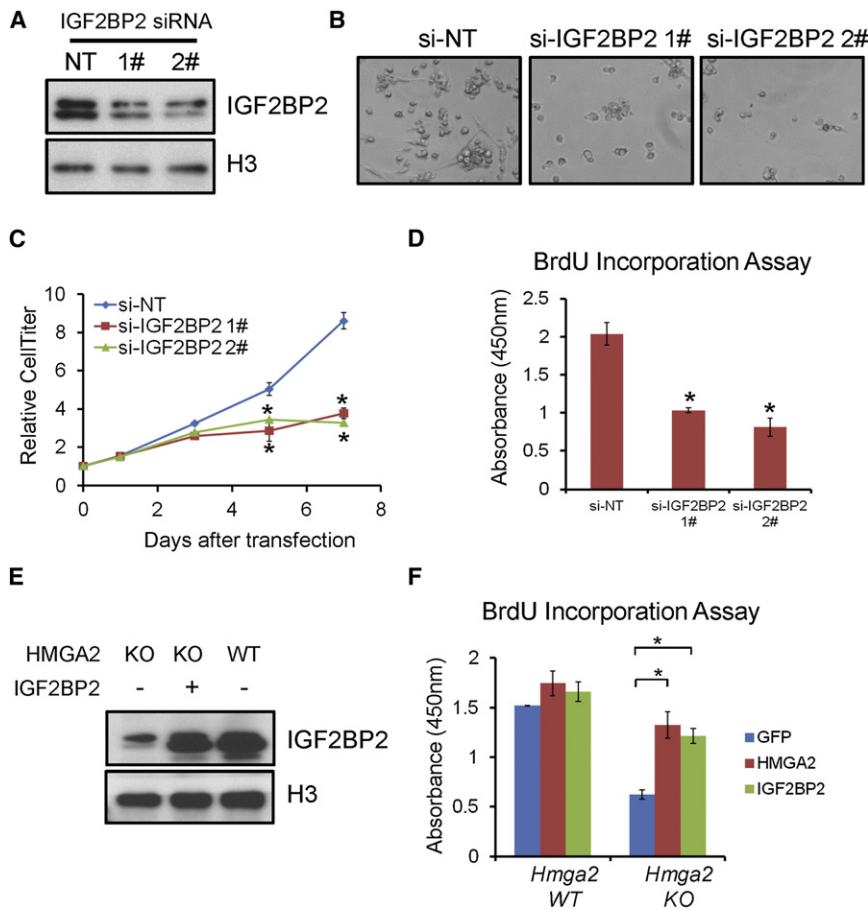
Figure 6. IGF2BP2 Is Important for Myoblast Growth and Could Partially Rescue the Growth Deficiency of Hmga2 KO Myoblasts

(A) Successful knockdown of IGF2BP2 using siRNAs in myoblasts. Two individual siRNAs against IGF2BP2 and one nontargeting (NT) control siRNA were transfected into myoblasts, and protein samples were harvested 3 days after transfection. Western blots were performed using antibodies against IGF2BP2 and Histone H3.

(B) Knockdown of IGF2BP2 in myoblasts decreases cell growth. A total of 200,000 myoblasts were seeded into each well of 6-well plates. Cells were transfected with NT or *Igf2bp2* siRNAs. Pictures were taken 5 days after transfection.

(C) Knockdown of IGF2BP2 in myoblasts decreases cell growth. A total of 10,000 myoblasts were seeded into each well of 96-well plates. Cells were transfected with NT or *Igf2bp2* siRNAs at day 0. Cell titers were measured at day 0, 1, 3, 5, and 7 after transfection by CellTiter-Glo Luminescent Cell Viability Assay kit (Promega). $p < 0.05$ versus si-NT samples at the same time point. Error bars depict mean ± SEM.

(D) Knockdown of IGF2BP2 in myoblasts decreases BrdU incorporation. Myoblasts were seeded into each well of 96-well plates. Cells were transfected with NT or *Igf2bp2* siRNAs at day 0. At day 5, BrdU assays were performed by BrdU Cell Proliferation Assay Kit (Cell Signaling Technology), according to the manufacturer's guidance. $p < 0.05$ versus si-NT samples. Error bars depict mean ± SEM.

(E) Overexpression of IGF2BP2 in *Hmga2* KO myoblasts. Lentivirus expressing IGF2BP2 were infected into *Hmga2* KO myoblasts. Three days after infection, protein samples were harvested. Western blots were performed using antibodies against IGF2BP2 and Histone H3.

(F) Overexpression of IGF2BP2 could partially rescue the proliferation deficiency of *Hmga2* KO myoblasts. A total of 5,000 *Hmga2* KO and WT myoblasts were seeded into each well of 96-well plates. Lentivirus expressing IGF2BP2 or HMGA2 was used to infect cells. BrdU assays were performed 5 days after infection. $p < 0.05$. Error bars depict mean ± SEM.

Surprisingly, $p16^{Ink4A}$ and $p19^{ARF}$, reported targets of HGMA2 in neural stem cells (Nishino et al., 2008), were not regulated by HMGA2 in myoblasts. Of all the downregulated genes, *Igf2bp2* is particularly interesting. First, it is the most significantly downregulated gene in *Hmga2* KO myoblasts, and two independent probes against *Igf2bp2* were identified among the top 5 regulated genes (Figures 5A and 5B). Second, *Igf2bp2* has a very similar expression pattern as *Hmga2* during myogenesis: low in quiescent satellite cells, strongly upregulated in myoblasts, and gradually downregulated during terminal differentiation (Figure 5C). These data strongly suggest HMGA2 may regulate *Igf2bp2* expression in myoblasts. qRT-PCR confirmed that *Igf2bp2* mRNA was significantly downregulated in *Hmga2* KO myoblasts (Figure 5D). Western blots demonstrated that IGF2BP2 protein was almost undetectable in *Hmga2* KO myoblasts (Figure 5E). Moreover, when HMGA2 was overexpressed in myoblasts, using a lentiviral construct, both *Igf2bp2* mRNA and protein levels increased (Figures 5F and 5G). All these data demonstrate that *Igf2bp2* is a downstream target for HMGA2 in myoblasts, and that HMGA2 is required for *Igf2bp2* protein to be made.

IGF2BP2 was previously reported to be potentially regulated by HMGA2 during embryonic development (Cleynen et al., 2007), although the biological significance of this regulation remained unclear. HMGA2 was shown to bind to the first intron of *Igf2bp2*, where it enhanced the binding of NF-κB factors such as p65 and p50 (Cleynen et al., 2007). To investigate whether this mechanism is conserved in myoblasts, chromatin immunoprecipitation was performed, and direct binding of HMGA2 and p65 to the *Igf2bp2* intron region was detected. By contrast, HMGA2 and p65 don't bind to either *Gapdh* promoter or *IgH* enhancer regions (Figure 5H).

IGF2BP2 Regulates Myoblast Proliferation, and Overexpressing IGF2BP2 Can Partially Rescue the Growth Deficiency of Hmga2 KO Myoblasts

The roles of IGF2BP2 in myogenesis or cell proliferation in general have not been studied. Therefore, we investigated whether the regulation of IGF2BP2 by HMGA2 is biologically relevant. siRNAs against *Igf2bp2* were used to knock down IGF2BP2 protein and they successfully reduced IGF2BP2 protein by 70%~80% (Figure 6A). Two independent *Igf2bp2*

siRNAs significantly decreased myoblast growth as measured by CellTiter assay (Figures 6B and 6C). They also caused a decrease in BrdU incorporation (Figure 6D), proving that a decline in IGF2BP2 reduced cell proliferation.

These data point to the possibility that the HMGA2 effect on myoblast proliferation could be at least partially mediated by IGF2BP2. To examine this, IGF2BP2 was overexpressed in *Hmga2* KO myoblasts. Western blots confirmed that IGF2BP2 overexpression restored the protein level, comparable to that in *Hmga2* WT myoblasts (Figure 6E). Importantly, overexpression of either HMGA2 itself or IGF2BP2 significantly increased the proliferation of *Hmga2* KO myoblasts (Figure 6F).

Taken together, these data indicate that IGF2BP2 is a functional target for HMGA2 in myoblasts, and that add-back of IGF2BP2 can largely rescue the HMGA2 null effect on myoblast proliferation.

IGF2BP2 Regulates the Protein Production of Multiple Genes Important for Cell Growth

We next investigated the molecular mechanism by which IGF2BP2 regulates myoblast growth. After binding to mRNAs, IGF2BPs reportedly can either positively or negatively regulate their translation (Christiansen et al., 2009). For example, IGF2BP2 could bind to *Igf2* mRNA and enhance its translation (Dai et al., 2011). We therefore asked whether IGF2BP2 controls myoblast proliferation by regulating the translating of mRNAs. By analyzing a public database (Hafner et al., 2010), exogenously overexpressed IGF2BP2 was found to bind to as many as 2,184 different mRNAs in 293 cells. Interestingly, the top 100 IGF2BP2 binding mRNAs are highly enriched in genes important for cell growth, including *c-myc*, *Sp1,* and *Igf1r* (Table S3). To examine whether endogenous IGF2BP2 also binds to these mRNAs in primary mouse myoblasts, RNA-binding protein immunoprecipitation was performed to pull down IGF2BP2 protein from a myoblast lysate, and the binding RNAs were determined. Many of the reported mRNAs were confirmed to be bound by endogenous IGF2BP2, including *c-myc, Sp1, Igf1r, Cyclin G1, Notch 2, Cdk6, Akt 3, Mdm2, Ki67, Arf1*, and *Mapk1*. By contrast, *Gapdh*, *Hdac1*, and *Smurf* mRNAs did not significantly bind to IGF2BP2 in myoblasts. Surprisingly, no strong binding of *Igf2* mRNA to IGF2BP2 was observed (Figure 7A).

To investigate whether IGF2BP2 could affect the translation of the determined target mRNAs, IGF2BP2 was knocked down by siRNA in myoblasts. Three days after transfection, western blots were performed to examine protein levels of the candidates determined by pull down. Protein levels of c-Myc, SP1 and IGF1R were significantly reduced upon IGF2BP2 siRNA treatment (Figure 7B). Interestingly, IGF2BP2 siRNA did not significantly change levels of *c-myc*, *Sp1*, and *Igf1r* mRNAs (Figure 7C), suggesting that IGF2BP2 knockdown could perturb protein levels of target mRNAs in myoblasts without affecting overall mRNA levels.

Because *Hmga2* KO myoblasts have significantly less IGF2BP2, the protein levels of IGF2BP2-required targets should also decrease in *Hmga2* KO myoblasts. Indeed, *Hmga2* KO myoblasts showed a significant reduction of c-Myc, SP1, and IGF1R proteins (Figure 7D). Similar to the previous *Igf2bp2* siRNA experiments, *c-myc*, *Sp1*, and *Igf1r* mRNAs were not

differentially expressed between *Hmga2* KO and WT myoblasts (Figure S6A). To directly assess whether mRNA translation is reduced in *Hmga2* KO myoblasts, polysome isolation experiments were performed (Figure S6B). Percentages of *c-myc*, *Sp1*, and *Igf1r* mRNAs associated with polysomes were all reduced in *Hmga2* KO myoblasts (Figure 7E), proving that their translation was inhibited. Because c-Myc, SP1, IGF1R, and many other targets all have well-known roles in cell growth and myogenesis, the downregulation of those proteins provide obvious potential explanations for the growth deficiency observed in *Hmga2* KO and *Igf2bp2* siRNA-treated myoblasts.

HMGA2 in Dystrophic and Aged Muscle

To investigate whether HMGA2 is perturbed in settings of Duchenne's muscular dystrophy or in sarcopenia (age-associated muscle atrophy and weakness), we first examined the levels of *Hmga2* in Mdx mice, a model for Duchenne's. mRNA samples were harvested from young (week 4), diseased (week 10), and old (week 50) Mdx and control mice. At various disease stages, *Hmga2* mRNA levels were all higher in Mdx muscles in comparison to WT controls (Figure 8A). This is consistent with the continuous cycle of degeneration/regeneration and myoblast proliferation in dystrophic muscles (Bulfield et al., 1984; Tanabe et al., 1986). This finding also suggests that simply increasing HMGA2 levels is unlikely to ameliorate the phenotype seen in this type of muscle dystrophy, because HMGA2 is already upregulated.

Aged muscle reportedly is coincident with a significant reduction in stem cell function (Brack and Rando, 2007; Day et al., 2010). To examine whether HMGA2 is involved in the sarcopenic phenotype, mRNAs were compared using a collection of human myoblasts of different ages. *Hmga2* mRNA levels were comparable in young and aged myoblasts (Figure 8B). However, differences were seen when the myoblasts were subject to differentiation; myoblasts from 20-year-old, 50-year-old, 73-year-old, and 83-year-old donors were grown to confluence and switched to differentiation conditions. While all samples had similar H*mga2* levels before differentiation, the myoblasts from the oldest population, 83 years, where sarcopenia is often evident, did not show a statistically significant difference between undifferentiated and differentiated levels of *Hmga2*, in contrast to the other age groups (Figure 8C); this is consistent with the finding that these myoblasts demonstrate delays and an overall deficiency in myoblast differentiation (data not shown). Interestingly, reduction of HMGA2 seems crucial for differentiation, because constitutive overexpression of HMGA2 in myoblasts inhibits terminal differentiation (Figure S7). Our data together demonstrate that reduced proliferation capacity of the most aged myoblasts is not correlated with *Hmga2* levels. However, the deficiency of shutting off *Hmga2* during differentiation might play a role in reduced myogenesis.

DISCUSSION

The activation and proliferation of skeletal muscle progenitor cells is one of the first required steps for muscle development and regeneration. The loss of the ability to regenerate muscle is part of the pathophysiology of muscular dystrophies (Blau, 2008) and has also been implicated as contributing to the
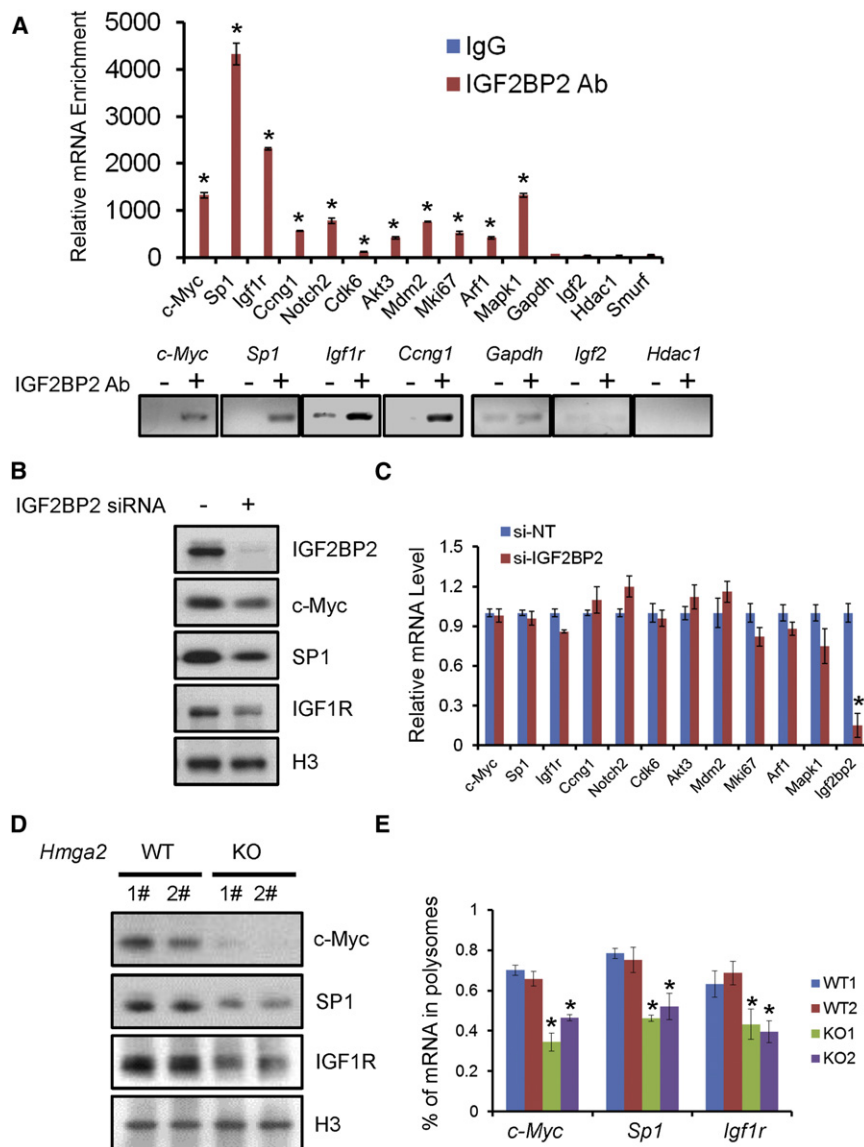
Figure 7. IGF2BP2 Binds to a Set of mRNAs and Regulates Protein Production

(A) IGF2BP2 binds to the mRNAs of genes involved in cell growth control. Immunoprecipitations were done using control IgG or IGF2BP2 antibodies Coimmunoprecipitated RNAs were eluted and analyzed by RT-PCR. IGF2BP2 strongly binds to the mRNAs of *c-Myc*, *Sp1*, *Igf1r* and several others, but not *Gapdh*, *Igf2*, *Hdac1*, and *Smurf* mRNAs. *p < 0.05 versus IgG control. Error bars depict mean ± SEM.

(B) Knockdown of IGF2BP2 decreases protein levels of c-Myc, SP1, and IGF1R. Myoblasts were transfected by *Igf2bp2* siRNAs for 4 days. Protein samples were harvested and western blots were performed using antibodies against IGF2BP2, c-Myc, SP1, IGF1R, and Histone H3.

(C) Knockdown of IGF2BP2 does not change the levels of top binding mRNAs. Myoblasts were transfected by IGF2BP2 or NT control siRNAs for 3 days. RT-PCR assays were performed using indicating primers. Data were normalized to *Gapdh* and *18 s* mRNAs. *p < 0.05 versus si-NT control. Error bars depict mean ± SEM.

(D) *Hmga2* KO myoblasts have decreased c-Myc, SP1 and IGF1R protein levels. Two WT and two KO myoblasts were cultured in proliferation medium. Protein samples were harvested and western blots were performed using antibodies against IGF2BP2, c-Myc, SP1, IGF1R, and Histone H3.

(E) Selective mRNAs associated with polysomes decrease in *Hmga2* KO myoblasts. Polysomes were isolated from *Hmga2* KO and WT myoblasts. Polysome mRNAs and total mRNAs were reverse transcribed and RT-PCR assays were performed using indicating primers. Data were normalized to *Gapdh* and *18 s* mRNAs. *p < 0.05 versus WT controls. Error bars depict mean ± SEM.

See also Figure S6 and Table S3.

loss of muscle mass associated with aging, termed sarcopenia (Brack and Rando, 2007; Conboy et al., 2005; Rüegg and Glass, 2011; Tanaka et al., 2009). Therefore, it is important to understand the molecular mechanisms controlling the early steps of myogenesis; toward this goal, we identified a group of genes that are highly and specifically expressed in proliferating myoblasts during muscle regeneration. Using both gain-of-function and loss-of-function assays, we identified HMGA2 to be a crucial regulator for muscle stem cell activation and myogenesis.

Pronounced loss of muscle mass and smaller muscle fibers in *Hmga2* KO mice demonstrates a critical requirement for HMGA2 in postnatal skeletal muscle development in vivo. Strong evidence is presented to show that reduced muscle progenitor activity leads to small muscle fibers in *Hmga2* KO mice. In contrast to skeletal muscle, other organs—including the heart and brain—are actually proportionally larger in *Hmga2* KO mice. This is noteworthy, because HMGA2 was previously re-

ported to be a crucial factor for heart development and neural stem cell self-renewal (Monzen et al., 2008; Nishino et al., 2008). The data also demonstrate that HMGA2 has nonredundant and unique roles compared to HMGA1 in skeletal muscle myoblasts. While *Hmga2* KO mice have a loss-of-skeletal muscle phenotype, *Hmga1* KO mice have normal body weight, as well as regular development of most major organs and tissues (Fedele et al., 2006).

Unlike what is reported in neural stem cells, HMGA2 does not seem to regulate p16^{Ink4A} or p19^{ARF} in myoblasts, which led us to seek other functional downstream factors. Through an unbiased microarray analysis, we identified IGF2BP2 as a key target and mediator for HMGA2's function in controlling myoblast proliferation. Although the regulation of IGF2BP2 by HMGA2 was reported in another cell system (Cleynen et al., 2007), the current study demonstrates that IGF2BP2 is crucial for cell proliferation and myogenesis, and that it mediates a large part of the HMGA2 effect on these muscle phenotypes.

IGF2BP2 acts by binding to and promoting the translation of various mRNAs. This function helps explain why HMGA2 and

Developmental Cell

Crucial Role of HMGA2 in Myogenesis
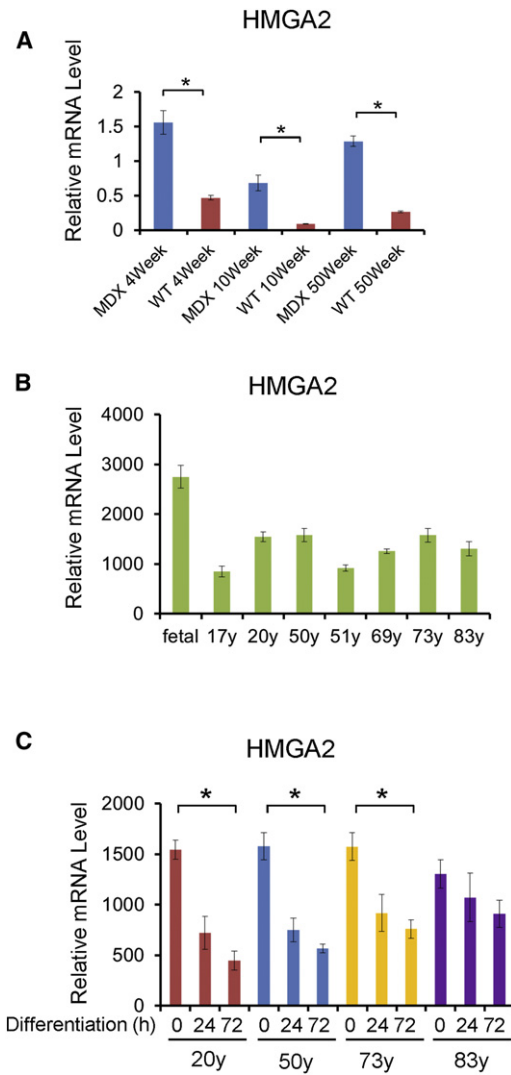
Figure 8. HMGA2 Is Dysregulated in Dystrophic and Aged Muscles
(A) *Hmga2* mRNA levels are higher in muscle samples isolated from Mdx mice than WT controls. RT-PCR assays were performed using *Hmga2* primers. Data were normalized to *Gapdh* and *18 s* mRNAs. *p < 0.05. Error bars depict mean ± SEM.
(B) *Hmga2* mRNA levels are similar in myoblasts of different ages. mRNAs were harvested from human myoblasts with different-aged donors. RT-PCR assays were performed using *Hmga2* primers. Data were normalized to *Gapdh* and *18 s* mRNAs. Error bars depict mean ± SEM.
(C) Impaired HMGA2 downregulation during differentiation in aged myoblasts. mRNA levels of HMGA2 were examined in human myoblasts isolated from different-aged donors (fetal to 83 years old). While there was no significant difference at day 0, a clear loss of HMGA2 downregulation during differentiation was observed only in cells from 83-year-old donors, where sarcopenia was most prevalent. *p < 0.05. Error bars depict mean ± SEM.
See also Figure S7.

IGF2BP2 are highly expressed in proliferating myoblasts, where transcription and translation are much more active than in quiescent stem cell or postmitotic myofibers. Given the large number of DNA binding sites for HMGA2, it is surprising that a single perturbed gene, in this case IGF2BP2, is responsible for much of the phenotype seen, but that seems to be the case

here. IGF2BP2 in turn binds many mRNAs, and we could at least confirm that the three target genes—*c-myc*, *Sp1*, and *Igf1r*—are all perturbed at the protein level. It will be of interest to investigate whether other mRNA targets were also affected in a similar manner.

The IGF1 pathway is well-established for its role in myoblast proliferation. IGF1 stimulates myoblasts to proliferate, but also has a biphasic role given its ability to stimulate differentiation (Florini et al., 1986; Quinn and Roh, 1993; Engert et al., 1996; Quinn et al., 1994). *Igf1* null animals are runted, as are *Igf1r* null animals (Liu et al., 1993), similar to the pygmy phenotype seen in the *Hmga2* nulls. Although c-*myc* is similar to IGF1 in that it can stimulate myoblast proliferation, c-*myc* has an opposite effect of IGF1 on differentiation: c-*myc*'s continued expression blocks differentiation (Miner and Wold, 1991) (La Rocca et al., 1994); thus, there is a requirement to downregulate c-*myc* late in myogenesis, which is what occurs with the downregulation of the HMGA2-IGF2BP2 axis. SP1 broadly interacts with other transcriptional factors or epigenetic regulators and has very important roles in early development and in cancer formation (Black et al., 2001). As for its role in myoblast proliferation, SP1 is least studied. One important myoblast proliferation-regulating protein that requires its SP1 binding elements to be expressed is the FGF receptor FGFR1 (Patel and DiMario, 2001). It will be of interest to further study FGF signaling perturbations in the *Hmga2* nulls, or the IGF2BP2 knockdown myoblasts.

In summary, the data presented here demonstrate that HMGA2 and IGF2BP2 are critical for myoblast proliferation and early myogenesis. When satellite cells are activated and enter the cell cycle, HMGA2 is upregulated and directly activates the transcription of *Igf2bp2*, which in turn positively controls the protein production of multiple proliferation related genes including *c-myc*, *Sp1*, and *Igf1r*. Not only is it necessary to upregulate HMGA2/IGF2BP2 for optimal proliferation, but it is also apparently required to downregulate HMGA2/IGF2BP2/c-Myc in order for myoblasts to be able to then differentiate into multinucleated skeletal muscle.

EXPERIMENTAL PROCEDURES

Animals

All procedures were performed in accordance with the standards of the US Department of Health and Human Services and were approved by the Novartis Animal Care and Use Committee. C57BL/6 mice and *Hmga2* +/− heterozygous mice (stock #002644) were obtained from Jackson Laboratories at 4∼6 weeks of age. Mice were housed and bred at Novartis Cambridge Lab Animal Services.

Muscle Regeneration

Muscle degeneration/regeneration by CTX was done as previously described (Palacios et al., 2010; Sherwood et al., 2004). In brief, left TA muscles of anesthetized 8- to 12-week-old C57BL/6 WT or *Hmga2* KO mice were intramuscularly injected with 100 μl of 10 μM CTX. Right TA muscles of the same mice were injected with PBS as control. Muscle samples were harvested for immunohistochemistry at day 0, day 3, day 7, and day 14 after injection and stained by H&E and specific antibodies. Regeneration is clearly activated in the first 3 days and recovered by 14 days after injury.

The muscle injury induction by frozen injury was performed according to previously described procedure (Warren et al., 2002). In brief, a small incision was made through aseptically prepared skin overlying the left TA muscle. Injury was induced by applying a steel probe cooled to the temperature of dry ice to the TA muscle for ∼10 s. Following injury, the skin incision was

closed using silk suture and treated with hydrogen peroxide. Muscle samples were harvested at day 5 after injury and we observed a mixture of regenerating and matured muscle fibers at this time point.

Single Fiber Cultures and Immunofluorescence
For single fiber cultures, EDL muscle was digested in 0.2% Collagenase type I (Invitrogen) in DMEM at 37°C and single fibers were gently triturated. Then, single fibers were carefully transferred into 10 ml of 5% horse serum (HS) in DMEM (Dulbecco's modified Eagle medium, GIBCO) and incubated at 37°C in 5% CO_2 for 15 min. This was repeated a minimum of three times to remove all bad and contracted fibers. Single fibers were then cultured in plating medium (10% HS, 0.5% chick embryo extract [CEE; US Biological, Swamp-scott, MA] in DMEM) for 1 day and then switched to proliferating medium (20% fetal bovine serum [Mediatech, Herndon, VA], 10% HS, 2% CEE in DMEM). Single fibers were fixed in 4% paraformaldehyde (PFA) for 10 min at room temperature, permeabilized (0.2% PBS/0.2% Triton X-100 [PBST]) and incubated in blocking solution (BS; 10% goat serum, PBST) for 30 min. Primary antibodies were incubated in BS overnight at 4°C. The day after single fibers were washed with PBST, incubated in BS for 30 min and in secondary antibodies and DAPI to visualize nuclei for 1 hr at room temperature. After several washes with PBST, single fibers were mounted and observed at fluorescence microscopy. Antibodies used were mouse anti-Pax7 (1/100, DSHB), rabbit anti-MyoD (1/70, Santa Cruz), and rabbit anti-Myogenin (1/200, Santa Cruz).

Myoblast Culture and Differentiation
Primary mouse satellite cells were isolated from C57BL/6 mice. Once isolated, satellite cells become activated and acquire myoblast property. To grow primary myoblast, cells were cultured in F10 (GIBCO) + 20% horse serum (GIBCO) + 2.5 ng/ml bFGF (Invitrogen) + 1% penicillin/streptomycin + 1% Gluta-Max (GIBCO). Human myoblast cells HSMM were obtained from Lonza (#CC-2580) and cultured with Clonetics Skeletal Muscle Myoblast Cell System (#CC-3245 and #CC-5034) for proliferation. When induced for differentiation, all three types of myoblast were switched from their perspective growth medium into fusion medium (DMEM/F12 supplemented with 2% horse serum). When induced for differentiation, myoblasts were switched to differentiation medium (DMEM supplemented with 5% horse serum).

Immunofluorescence and Immunohistochemistry
Staining of frozen muscle sections (8 mm thick) was performed as previously described (Sherwood et al., 2004). Briefly, H&E staining was done by standard protocol. For immunofluorescence, frozen sections or cells grown in chamber slides were fixed in 4% PFA for 15 min in room temperature and permeabilized by 0.5% Triton X-100. Samples were then stained with primary antibody for 2 hr and with secondary antibody for 30 min at room temperature. Nuclei were labeled with DAPI. Primary antibodies used are HMGA2 (Cell Signaling #5269), MHC (Millipore, #05-833), Desmin (Cell Signaling #4024), Laminin (Abcam, #ab11576), and Pax7 (DSHB and a gift of Chen-Ming Fan). The secondary antibodies used are all from Invitrogen.

RNA-Binding Protein Immunoprecipitation
RNA-binding protein immunoprecipitation (RIP) was performed using Magna RIP RNA-Binding Protein Immunoprecipitation Kit (Millipore). Briefly, primary mouse myoblasts were harvested by adding RIP lysis buffer. Clear superna-tant containing IGF2BP2 protein, IgA beads, and IGF2BP2 antibody (or IgG control) were mixed to perform immunoprecipitation. After washing, RNAs binding to IGF2BP2 were eluted and quantified. Reverse transcription and RT-PCR were performed to examine whether certain mRNAs were coimmuno-precipitated with IGF2BP2 antibody.

Signature Analysis
Proliferation Signature is analyzed and modified from published data (Fukada et al., 2007). A total of 642 genes were identified to be upregulated more than 5 times at mRNA level in myoblast in comparison to quiescent satellite cells (see Table S1 for full gene list). Differentiation Signature is reanalyzed and modified from data previously published by Novartis (Gene Expression Omnibus [GEO] number GSE11415). A total of 328 genes show steady decrease during myo-differentiation and dropped by more than 80% at day 5.

Statistical Analyses
Descriptive statistics were generated for all quantitative data with presentation of means and standard errors. Results were assessed for statistical signifi-cance using Student's t test (Microsoft Excel) or ANOVA analysis using the SAS Enterprise Guide 3.0 or SigmaPlot 11.0 software.

ACCESSION NUMBERS

The GEO database accession number for the microarray reported in this paper is GSE41907.

SUPPLEMENTAL INFORMATION

Supplemental Information includes seven figures, three tables, and Supple-mental Experimental Procedures, and can be found with this article online at http://dx.doi.org/10.1016/j.devcel.2012.10.019.

REFERENCES

Anand, A., and Chada, K. (2000). In vivo modulation of Hmgic reduces obesity. Nat. Genet. 24, 377–380.

Ashar, H.R., Chouinard, R.A., Jr., Dokur, M., and Chada, K. (2010). In vivo modulation of HMGA2 expression. Biochim. Biophys. Acta 1799, 55–61.

Black, A.R., Black, J.D., and Azizkhan-Clifford, J. (2001). Sp1 and krüppel-like factor family of transcription factors in cell growth regulation and cancer. J. Cell. Physiol. 188, 143–160.

Blau, H.M. (2008). Cell therapies for muscular dystrophy. N. Engl. J. Med. 359, 1403–1405.

Bodine, S.C., Latres, E., Baumhueter, S., Lai, V.K., Nunez, L., Clarke, B.A., Poueymirou, W.T., Panaro, F.J., Na, E., Dharmarajan, K., et al. (2001). Identification of ubiquitin ligases required for skeletal muscle atrophy. Science 294, 1704–1708.

Brack, A.S., and Rando, T.A. (2007). Intrinsic changes and extrinsic influences of myogenic stem cell function during aging. Stem Cell Rev. 3, 226–237.

Bulfield, G., Siller, W.G., Wight, P.A., and Moore, K.J. (1984). X chromosome-linked muscular dystrophy (mdx) in the mouse. Proc. Natl. Acad. Sci. USA 81, 1189–1192.

Caron, L., Bost, F., Prot, M., Hofman, P., and Binétruy, B. (2005). A new role for the oncogenic high-mobility group A2 transcription factor in myogenesis of embryonic stem cells. Oncogene 24, 6281–6291.

Christiansen, J., Kolte, A.M., Hansen, T.O., and Nielsen, F.C. (2009). IGF2 mRNA-binding protein 2: biological function and putative role in type 2 diabetes. J. Mol. Endocrinol. 43, 187–195.

Cleynen, I., Brants, J.R., Peeters, K., Deckers, R., Debiec-Rychter, M., Sciot, R., Van de Ven, W.J., and Petit, M.M. (2007). HMGA2 regulates transcription of the Imp2 gene via an intronic regulatory element in cooperation with nuclear factor-kappaB. Mol. Cancer Res. 5, 363–372.

Conboy, I.M., Conboy, M.J., Wagers, A.J., Girma, E.R., Weissman, I.L., and Rando, T.A. (2005). Rejuvenation of aged progenitor cells by exposure to a young systemic environment. Nature 433, 760–764.

Dai, N., Rapley, J., Angel, M., Yanik, M.F., Blower, M.D., and Avruch, J. (2011). mTOR phosphorylates IMP2 to promote IGF2 mRNA translation by internal ribosomal entry. Genes Dev. 25, 1159–1172.

Day, K., Shefer, G., Shearer, A., and Yablonka-Reuveni, Z. (2010). The depletion of skeletal muscle satellite cells with age is concomitant with reduced capacity of single progenitors to produce reserve progeny. Dev. Biol. 340, 330–343.

Engert, J.C., Berglund, E.B., and Rosenthal, N. (1996). Proliferation precedes differentiation in IGF-I-stimulated myogenesis. J. Cell Biol. 135, 431–440.

Fedele, M., and Fusco, A. (2010). HMGA and cancer. Biochim. Biophys. Acta 1799, 48–54.

Fedele, M., Fidanza, V., Battista, S., Pentimalli, F., Klein-Szanto, A.J., Visone, R., De Martino, I., Curcio, A., Morisco, C., Del Vecchio, L., et al. (2006). Haploinsufficiency of the Hmga1 gene causes cardiac hypertrophy and myelo-lymphoproliferative disorders in mice. Cancer Res. 66, 2536–2543.

Florini, J.R., Ewton, D.Z., Falen, S.L., and Van Wyk, J.J. (1986). Biphasic concentration dependency of stimulation of myoblast differentiation by somatomedins. Am. J. Physiol. 250, C771–C778.

Fukada, S., Uezumi, A., Ikemoto, M., Masuda, S., Segawa, M., Tanimura, N., Yamamoto, H., Miyagoe-Suzuki, Y., and Takeda, S. (2007). Molecular signature of quiescent satellite cells in adult skeletal muscle. Stem Cells 25, 2448–2459.

Hafner, M., Landthaler, M., Burger, L., Khorshid, M., Hausser, J., Berninger, P., Rothballer, A., Ascano, M., Jr., Jungkamp, A.C., Munschauer, M., et al. (2010). Transcriptome-wide identification of RNA-binding protein and microRNA target sites by PAR-CLIP. Cell 141, 129–141.

La Rocca, S.A., Crouch, D.H., and Gillespie, D.A. (1994). c-Myc inhibits myogenic differentiation and myoD expression by a mechanism which can be dissociated from cell transformation. Oncogene 9, 3499–3508.

Le Grand, F., and Rudnicki, M.A. (2007). Skeletal muscle satellite cells and adult myogenesis. Curr. Opin. Cell Biol. 19, 628–633.

Li, A.Y., Lin, H.H., Kuo, C.Y., Shih, H.M., Wang, C.C., Yen, Y., and Ann, D.K. (2011). High-mobility group A2 protein modulates hTERT transcription to promote tumorigenesis. Mol. Cell. Biol. 31, 2605–2617.

Liu, J.P., Baker, J., Perkins, A.S., Robertson, E.J., and Efstratiadis, A. (1993). Mice carrying null mutations of the genes encoding insulin-like growth factor I (Igf-1) and type 1 IGF receptor (Igf1r). Cell 75, 59–72.

Miner, J.H., and Wold, B.J. (1991). c-myc inhibition of MyoD and myogenin-initiated myogenic differentiation. Mol. Cell. Biol. 11, 2842–2851.

Monzen, K., Ito, Y., Naito, A.T., Kasai, H., Hiroi, Y., Hayashi, D., Shiojima, I., Yamazaki, T., Miyazono, K., Asashima, M., et al. (2008). A crucial role of a high mobility group protein HMGA2 in cardiogenesis. Nat. Cell Biol. 10, 567–574.

Nishino, J., Kim, I., Chada, K., and Morrison, S.J. (2008). Hmga2 promotes neural stem cell self-renewal in young but not old mice by reducing p16Ink4a and p19Arf Expression. Cell 135, 227–239.

Olguin, H.C., and Olwin, B.B. (2004). Pax-7 up-regulation inhibits myogenesis and cell cycle progression in satellite cells: a potential mechanism for self-renewal. Dev. Biol. 275, 375–388.

Palacios, D., Mozzetta, C., Consalvi, S., Caretti, G., Saccone, V., Proserpio, V., Marquez, V.E., Valente, S., Mai, A., Forcales, S.V., et al. (2010). TNF/p38α/polycomb signaling to Pax7 locus in satellite cells links inflammation to the epigenetic control of muscle regeneration. Cell Stem Cell 7, 455–469.

Patel, S.G., and DiMario, J.X. (2001). Two distal Sp1-binding cis-elements regulate fibroblast growth factor receptor 1 (FGFR1) gene expression in myoblasts. Gene 270, 171–180.

Pfannkuche, K., Summer, H., Li, O., Hescheler, J., and Dröge, P. (2009). The high mobility group protein HMGA2: a co-regulator of chromatin structure and pluripotency in stem cells? Stem Cell Rev. 5, 224–230.

Quinn, L.S., and Roh, J.S. (1993). Overexpression of the human type-1 insulin-like growth factor receptor in rat L6 myoblasts induces ligand-dependent cell proliferation and inhibition of differentiation. Exp. Cell Res. 208, 504–508.

Quinn, L.S., Steinmetz, B., Maas, A., Ong, L., and Kaleko, M. (1994). Type-1 insulin-like growth factor receptor overexpression produces dual effects on myoblast proliferation and differentiation. J. Cell. Physiol. 159, 387–398.

Rudnicki, M.A., Le Grand, F., McKinnell, I., and Kuang, S. (2008). The molecular regulation of muscle stem cell function. Cold Spring Harb. Symp. Quant. Biol. 73, 323–331.

Rüegg, M.A., and Glass, D.J. (2011). Molecular mechanisms and treatment options for muscle wasting diseases. Annu. Rev. Pharmacol. Toxicol. 51, 373–395.

Sherwood, R.I., Christensen, J.L., Conboy, I.M., Conboy, M.J., Rando, T.A., Weissman, I.L., and Wagers, A.J. (2004). Isolation of adult mouse myogenic progenitors: functional heterogeneity of cells within and engrafting skeletal muscle. Cell 119, 543–554.

Tanabe, Y., Esaki, K., and Nomura, T. (1986). Skeletal muscle pathology in X chromosome-linked muscular dystrophy (mdx) mouse. Acta Neuropathol. 69, 91–95.

Tanaka, K.K., Hall, J.K., Troy, A.A., Cornelison, D.D., Majka, S.M., and Olwin, B.B. (2009). Syndecan-4-expressing muscle progenitor cells in the SP engraft as satellite cells during muscle regeneration. Cell Stem Cell 4, 217–225.

Warren, G.L., Hulderman, T., Jensen, N., McKinstry, M., Mishra, M., Luster, M.I., and Simeonova, P.P. (2002). Physiological role of tumor necrosis factor alpha in traumatic muscle injury. FASEB J. 16, 1630–1632.

Watanabe, S., Ueda, Y., Akaboshi, S., Hino, Y., Sekita, Y., and Nakao, M. (2009). HMGA2 maintains oncogenic RAS-induced epithelial-mesenchymal transition in human pancreatic cancer cells. Am. J. Pathol. 174, 854–868.

Zammit, P.S., Golding, J.P., Nagata, Y., Hudon, V., Partridge, T.A., and Beauchamp, J.R. (2004). Muscle satellite cells adopt divergent fates: a mechanism for self-renewal? J. Cell Biol. 166, 347–357.

Supplemental Information

An HMGA2-IGF2BP2 Axis Regulates

Myoblast Proliferation and Myogenesis

Zhizhong Li, Jason A. Gilbert, Yunyu Zhang, Minsi Zhang, Qiong Qiu, Krishnan Ramanujan, Tea Shavlakadze, John K. Eash, Annarita Scaramozza, Matthew M. Goddeeris, David G. Kirsch, Kevin P. Campbell, Andrew S. Brack, and David J. Glass

Inventory of Supplemental Information

Supplemental Figures 1-7

Figure S1. Identification of signature genes in activated and proliferating myoblasts.

Figure S2, related to Figure 1. HMGA2 is highly expressed in skeletal muscle progenitors and decreases during differentiation.

Figure S3, related to Figure 2. Hmga2 KO mice demonstrate selective depletion of skeletal muscle and fat tissues.

Figure S4, related to Figure 3. HMGA2 regulates muscle development without regulating classic atrophy E3-ligases.

Figure S5, related to Figure 4. HMGA2 is not required for muscle terminal differentiation.

Figure S6, related to Figure 7. Translation of selective mRNAs are reduced in Hmga2 KO mice.

Figure S7, related to Figure 8. Overexpression of HMGA2 blocks terminal muscle differentiation.

Supplemental Tables 1-3

Table S1. Full list of genes in proliferating myoblast signature.

Table S2. Top genes regulated by HMGA2 in myoblasts.

Table S3. Top 100 IGF2BP2 binding mRNAs in 293 cells.
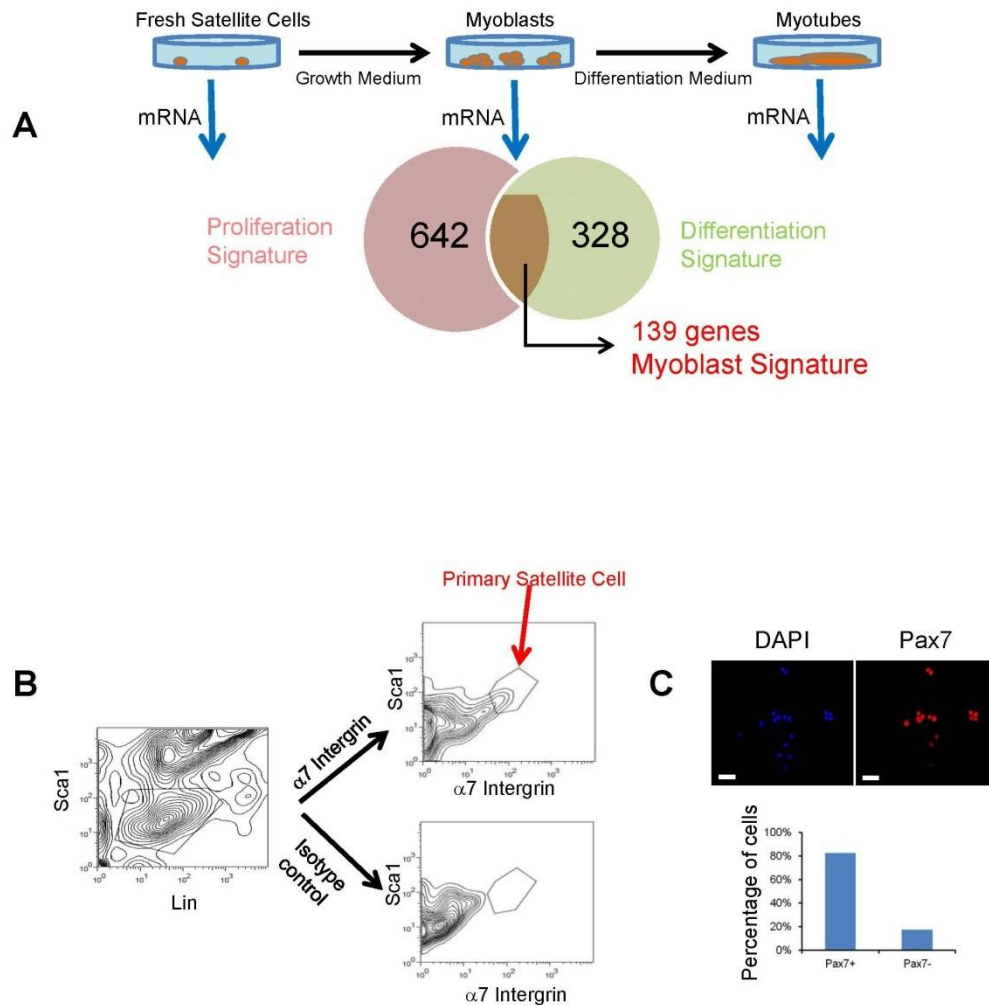
Supplemental Experimental Procedures

Figure S1: Identification of signature genes in activated and proliferating myoblasts.

(A) Microarray data identifies genes that are highly expressed in proliferating myoblasts, but not in satellite cells or differentiated myofibers. The "Proliferation Signature" consists of 642 genes whose mRNA levels were up-regulated at least 5 fold in proliferating myoblasts in comparison to satellite cells. The "Differentiation Signature" consists of 328 genes whose mRNA levels were down-regulated during muscle differentiation and reduced by at least 80% by day 5 after differentiation was

initiated.   The 139 individual genes in common between these two signatures are defined as constituting the "Myoblast Signature".

(B) Skeletal muscle fiber-associated cells were isolated and single cells were analyzed by flow cytometry. Satellite cells were enriched and isolated by a combination of surface markers: Sca1-CD45-Ter119-Mac1-α7 Integrin+. Gates were drawn based on FMO (Fluorescence Minus One) samples.

(C) Satellite cells were sorted into laminin-coated 96 well plates and cultured in growth medium supplied containing serum and bFGF for 4 days. >80% cells were stained for myoblasts markers Pax7.
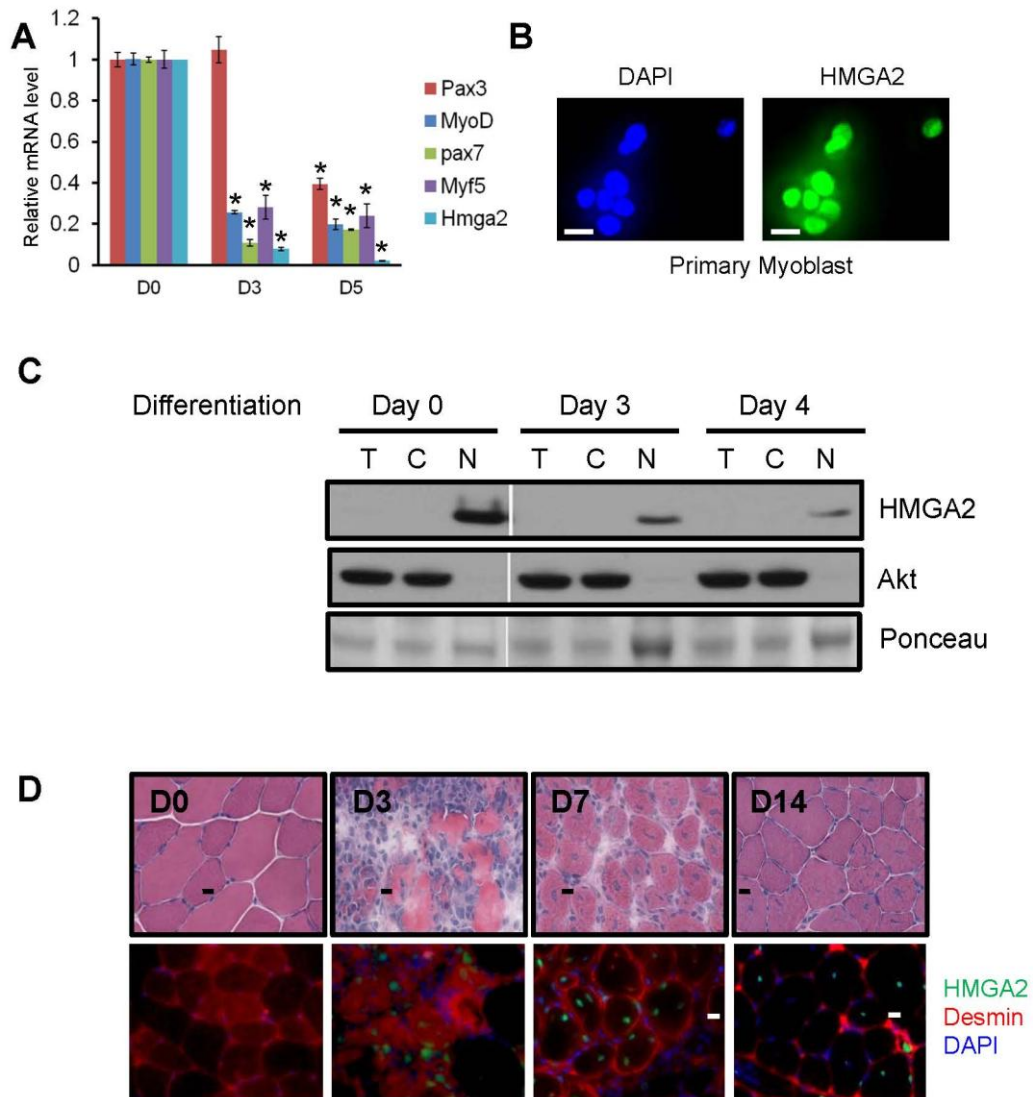
Figure S2: HMGA2 is highly expressed in skeletal muscle progenitors and decreases during differentiation

(A) *Hmga2* mRNA levels quickly dropped during primary myoblasts differentiation. Primary myoblasts were cultured in grow media to reach 80% confluence and switched into differentiation medium for up to 5 days. mRNA samples were harvested at day 0, day 3, and day 5 during

differentiation. RT-PCR was then performed against Hmga2 and myoblast markers *Pax3*, *Pax7*, *MyoD* and *Myf5*. Data were normalized to *Gapdh* and *18s* mRNAs. * p<0.05 versus mRNA level at day 0. Error bars depict mean ± SEM.

(B) Immunofluorescence demonstrates that HMGA2 protein is highly expressed in primary mouse myoblasts. Primary mouse myoblasts were fixed and stained for HMGA2 and DAPI. 80%~90% myoblast nuclei were stained positive for HMGA2 (scale bar: 10μm).

(C) HMGA2 protein level gradually decreases during C2C12 myoblast differentiation. 80% confluent C2C12 myoblasts were cultured in differentiation medium for 5 days. Total cell lysate, cytoplasmic and nuclear fractionated proteins were harvested at day 0, day 3 and day 5. Western blots were performed using antibodies against HMGA2, total AKT and Alpha-Tubulin (loading control). T=total cell lysate, C=cytoplasmic fraction, N=nuclear fraction.

(D) HMGA2 is absent in adult muscle tissue but re-activated during muscle regeneration. Cardiotoxin was injected into the tibialis anterior (TA) muscles of 8 week old C57BL/6 mice and muscle samples were harvested at day 0, day 3, day 7 and day 14 after injection for paraffin or frozen embedding. Samples were sectioned and stained for H&E, HMGA2, Desmin and DAPI. H&E staining proved that muscle regeneration occurred as expected, evident by massive inflammation and tissue necrosis at day 3, the existence of centralized nuclei at day 7 and reappearance of mature myofibers at day 14. Consistent with previous Western blot results, HMGA2 was almost undetectable at day 0. However, at day 3 after muscle injury, HMGA2 protein level was strongly boosted in muscle tissues. Its expression was slightly decreased but maintained in the centralized nuclei at day 7. After day 14, when many muscle fibers had been repaired and matured, the HMGA2 protein level dropped (scale bar: 10μm).
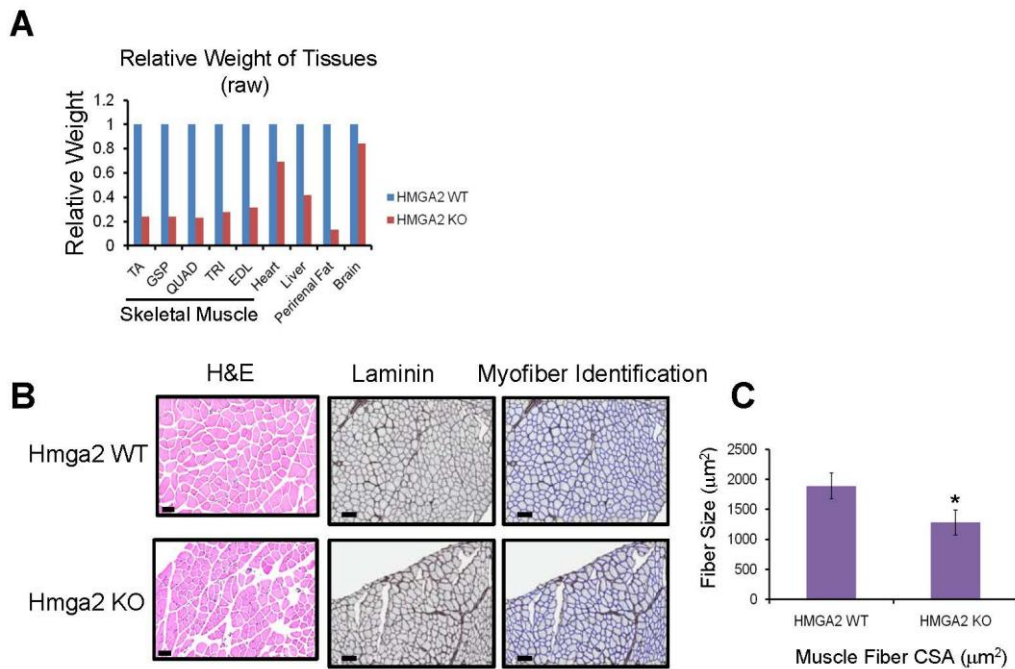
Figure S3: Hmga2 KO mice demonstrate selective depletion of skeletal muscle and fat tissues

(A) Quantification of raw weight of various tissues from *Hmga2* KO and WT mice indicated that all checked organs/tissues were significantly smaller in *Hmga2* KO mice. Tissues include skeletal muscle (TA, GSP, QUAD, TRI, and EDL), heart, liver, perirenal fat and brain. TRI=tricep, EDL=Extensor Digitorum Longus.

(B) H&E and Laminin staining of cross sections of *Hmga2* KO and WT muscle. Muscle fibers were identified by software Astoria v3.0, developed at Novartis Institutes for Biomedical Research. Cross section area data (CSA) was then analyzed by Astoria.

(C) Cross section area (CSA) is significantly smaller in *Hmga2* KO mice. The average fiber size was 1250 μm^2 (KO) versus 1820 μm^2 (WT). * $p<0.05$ versus Hmga2 WT. Error bars depict mean $\pm$ SEM.
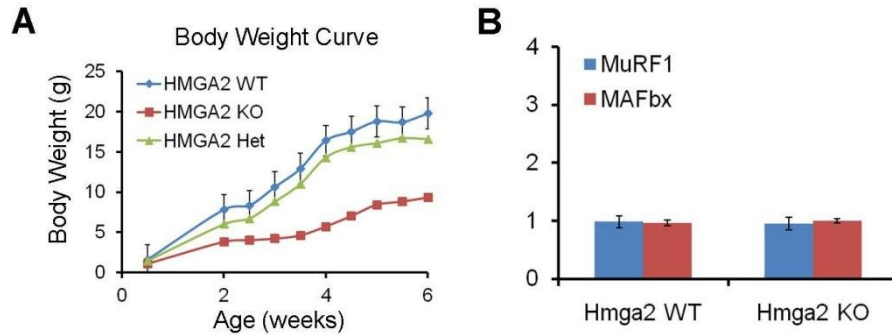
Figure S4: HMGA2 regulates muscle development without regulating classic atrophy E3-ligases

(A) *Hmga2* KO mice grew significantly slower than WT or Het littermates. The body weights of *Hmga2* KO, Het and WT mice were measured every 3~4 days between week 1 and week 6.

(B) *MuRF1* and *MAFbx* mRNA levels were not changed in *Hmga2* WT and *Hmga2* KO mice, suggesting the muscle atrophy we observed in *Hmga2* KO mice was not driven by these E3 ubiquitin ligases. Error bars depict mean ± SEM.
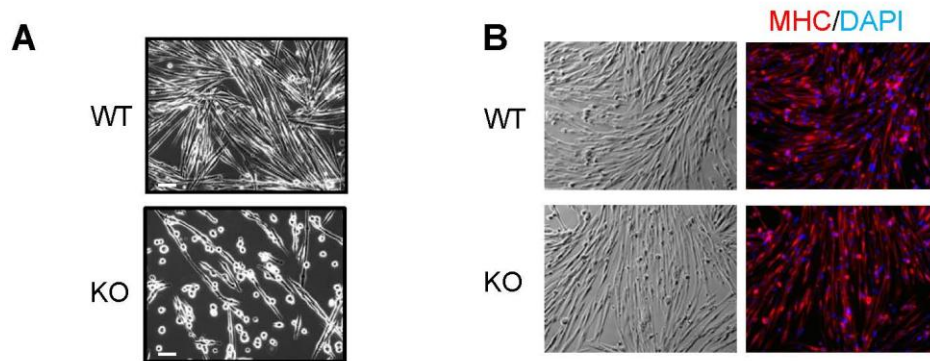
Figure S5: HMGA2 is not required for muscle terminal differentiation

(A) *Hmga2* KO myoblasts had reduced differentiation when cells were seeded at low density. 10,000 myoblasts from *Hmga2* KO and WT mice were seeded into each well of 96-well plates. Cells were cultured in proliferation medium for 2 day before switched into differentiation medium. Pictures were taken 3 days after inducing differentiation.

(B) *Hmga2* KO and WT myoblasts differentiated similarly when cells were seeded at high density. 50,000 myoblasts from *Hmga2* KO and WT mice were seeded into each well of 96-well plates. Cells were directly cultured in differentiation medium. Pictures were taken 2 days after inducing differentiation.

A

Hmga2 Myoblasts

Relative mRNA Level

- WT1
- WT2
- KO1
- KO2

c-Myc   Sp1   Igf1r

B

WT   KO

Polysome Isolation

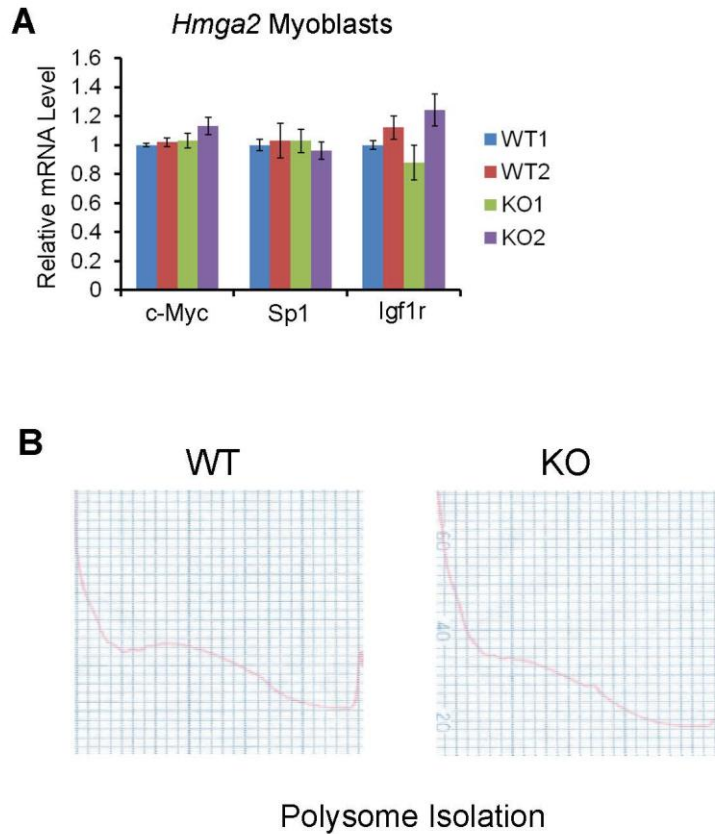*Figure S6: Translation of selective mRNAs are reduced in Hmga2 KO mice*

(A) mRNA levels of *c-Myc*, *Sp1* and *Igf1r* are similar between *Hmga2* KO and WT myoblasts. 2 WT and 2 KO myoblasts were cultured in proliferation medium. RT-PCR assays were performed using indicating primers. Data were normalized to *Gapdh* and *18s* mRNAs. Error bars depict mean ± SEM.

(B) Polysome isolation from WT and KO myoblasts.
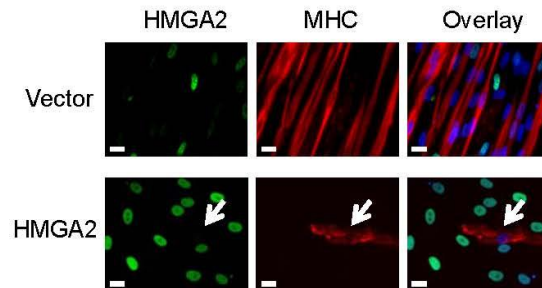
Figure S7: Overexpression of HMGA2 blocks terminal muscle differentiation

Human myoblasts were infected by lentiviral based HMGA2 overexpression or vector only constructs for 48 hours and switched to differentiation medium for another 72 hours. Cells were then fixed and stained with HMGA2, MHC and DAPI antibodies for Immunofluorescence. HSMM cells infected with vector control showed diminished HMGA2 and strong HMC staining after inducing differentiation. In contrast, cells infected with HMGA2 construct had sustained HMGA2 nuclear staining. Importantly, overexpression of HMGA2 in HSMM led to clear reduction of MHC-positive cells, in comparison to control samples (scale bar: 10μm).

Table S1: Full list of genes in proliferating myoblast signature

Gene Symbols of 139 independent genes in Proliferating Myoblast Signature.

Hmga2	Ccna2	Mad2l1	Mki67
Gzme	Acot7	Top2a	Nusap1
Rrm2	Tacc3	Mcm10	Lig1
Cdc25c	Melk	Hells	Stmn1
Kcnn4	Kntc2	Zwilch	Cks2
E2f8	2810433K01Rik	Kif23	Chek1
Ccnb1-rs1	6720460F02Rik	Dut	Foxm1
Ppil5	Prc1	4632417K18Rik	2700094K13Rik
Gtse1	Cdca5	Pole	Pcolce2
Ccnf	Cdc20	Ect2	Rbl1
Ube2c	Tpx2	Smc2	Dhfr
Ncapg	Racgap1	Asf1b	F730047E07Rik
Tk1	Dbf4	Rad54l	Dtl
Ccnb1	Ttk	Cenpf	Nasp
Cst6	Anln	C79407	Rcc1
Sgol1	Cks1b	Hmgb2	Cklf
Uhrf1	Cenpa	Mcm3	Arl6ip1
Ccdc99	Fabp5	Bub1b	1700054N08Rik
Kif2c	Nuf2	2610510J17Rik	BC025007
Bub1	Tyms	Gclm	Timeless
Kif22	Shcbp1	Ccne2	Aspm
MGC73635	Dlg7	Ckap2	Chtf18
Trip13	Spbc25	Kif11	Exo1
Diap3	Brca1	Prim1	C330027C09Rik
Spag5	Ercc6l	Ncapd2	Rad51
Hmmr	2810417H13Rik	D17H6S56E-5	Rfc3
Aurka	Plk4	Ccnb2	Birc5
Cdc2a	Mcm5	Ncaph	AW049604
Fignl1	Aurkb	Mcm2	Plk1
Rad51ap1	Cenpk	Kif18a	Ada
Eme1	Tubb3	Tmem48	Mybl2
Cep55	Incenp	Gins1	Pqlc2
Igfbp2	Cdca3	Fosl1	Cdt1
Cdc6	Fen1	Chaf1b	Kif20a
Gmnn	Pbk		

Table S2: Top genes regulated by HMGA2 in myoblasts

Gene Symbols of 28 significantly down-regulated and 30 significantly up-regulated genes in *Hmga2* KO myoblasts, in comparison to WT samples.

Gene	myoblast.logFC	Gene	myoblast.logFC
Igf2bp2	-1.669312121	Gpr123	1.008874947
Lmcd1	-1.554570521	Pcdh17	1.035791209
Myh8	-1.465920729	Ripk3	1.042871456
Bex1	-1.463225927	Lrrn3	1.05278992
Zdbf2	-1.462059911	Pcsk2	1.062531182
Esrrg	-1.444932094	Prr5l	1.066993348
Ankrd2	-1.432361186	Lipo1	1.067935016
C79818	-1.358768711	Cyyr1	1.123758729
Fn3k	-1.353508988	Ces2g	1.14317053
Pdlim4	-1.31814465	Pid1	1.155730913
Fabp3	-1.31225086	Mmp23	1.177072074
Capn3	-1.297823378	Rbm47	1.211088472
Acsl6	-1.278285756	Pcsk2	1.219346984
Cox8b	-1.232821797	Mmp23	1.220382913
Ccdc162	-1.210658884	Selp	1.239571522
Colec10	-1.206840274	Oxtr	1.345203596
Pacsin3	-1.176935039	Cthrc1	1.395706895
Reep1	-1.152731357	Pcsk2	1.398099023
2310046A06Rik	-1.119810207	Pcdhb20	1.438661089
4933404I11Rik	-1.114857257	Cldn1	1.479935466
Ptgis	-1.090671582	Stmn2	1.498802943
Lman1l	-1.088535147	Car8	1.609529808
Lpar3	-1.078997557	Sostdc1	1.653222607
Ankrd23	-1.077792243	Sp6	1.708637598
Mfsd4	-1.059727341	Tcrb-J	1.727624697
Klhl30	-1.028578605	Smoc2	1.740344321
Gpr155	-1.018890713	Lgr6	1.748251283
Adssl1	-1.00401193	Eya2	1.751877704
		1700091H14Rik	1.755246098
		Scd1	1.766102825

Table S3: Top 100 IGF2BP2 binding mRNAs in 293 cells

Gene Symbols of 100 mRNAs most significantly bound by IGF2BP2 in 293 cells.

NUCKS1	SRSF1	MED13	PCBP2
PEG10	MYC	TAOK1	NUDT21
TOMM20	PTP4A1	NRAS	CCT2
TMED2	CCNG1	ADNP	ICMT
CBX5	PTPLAD1	PROSER1	JMY
RPL15	CLIC4	ANKRD40	UHMK1
XIST	YARS	UBXN2B	CDK6
TMBIM6	SRCAP	IGF1R	FHL1
NUFIP2	KLHL15	PRRC2C	CERS2
PGAM5	CANX	QSER1	MLL5
SRRM2	SP1	LCOR	PPPDE1
SERBP1	SCD	LARP1	TEX261
AKT3	ZNF146	SLC7A1	GRPEL2
MAP1B	H3F3B	C5orf51	HNRNPUL1
TMPO	ARPP19	PAICS	ERH
MDM2	TUBB	PURB	NR3C1
TUG1	SLC38A2	WNK1	NOTCH2
MUC16	CALU	RMND5A	LRRC58
ZNF664	CAPZA1	FSTL1	RLIM
CCND2	SCML1	YWHAE	ANP32A
EIF1	SLC38A1	ZNF829	TOR1AIP2
GLO1	GNG12	FAM208B	CSNK2A1
MKI67	ARF1	BCLAF1	JAGN1
EEF2	CDK6	HSP90AA1	RPL18
KPNA6	HNRNPU	MAPK1	AP3M1

Supplemental Experimental Procedures

Genotyping

All mice were genotyped by PCR using following primers at 2~3 weeks of age:

Gene	Foward Primer	Reverse Primer
Hmga2 WT	5'-CCCACTGCTCTGTTCCTTGC-3'	5'-GTGTCCCTTGAAATGTTAGGCGGGG-3'
Hmga2 KO	5'-ATTCTGGAGACGCAGGAAGA-3'	5'-TGCTCCTGGGAGTAGATTGG-3'

CellTiter assays

Cells were infected by HMGA2 or NT shRNA virus for 48 hours. 5,000 cells were then seeded into each well of 96-well plates. Cell titers were determined after the indicated number of days using the CellTiter-Glo Luminescent Cell Viability Assay kit (Promega).

Chromatin immunoprecipitation

Active Motif's ChIP-IT® Express Kit was used for Chromatin Immunoprecipitation experiment according manufacture's instructions. Briefly, Cells were cross-linked with 1% formaldehyde for 10 min at room temperature and lysed in SDS lysis buffer. Samples were then sonicated or enzymatically digested to obtain DNA fragments with an average length of 200-800 bp. Supernatant containing DNA-protein complex were used for immunoprecipitations using HMGA2 antibody or normal rabbit IgG control. Immunoprecipitated chromatin was collected using protein G magnet beads and, after washing and elution, reverse crosslinking was carried out with 0.2M NaCl at 65°C overnight. The chromatin was then digested by 20 μg of Proteinase K (Invitrogen) for 1h at 45°C and isolated by phenolchloroform extraction. PCR reactions were performed using SYBR Green PCR Master Mix (Applied Biosystems) and primers against *Gapdh* promoter, *IgH* enhancer and *Igf2bp2* intron were used. Data were normalized to input signal and reported to IgG values.

Satellite cell isolation and activation

Satellite cells were isolated as described by Sherwood and colleagues (2004). Hindlimb muscles (extensor digitorum longus, gastrocnemius, quadriceps, hamstrings, soleus, and tibialis anterior) were digested in 0.2% Collagenase Type II (Gibco) in DMEM at 37 degree for 1.5 hours. Intact myofibers were then separated by vigorous pipetting, followed by centrifugation/gravitational separation. The myofiber pellet was further digested with 0.0125% Collagenase Type II and 0.05% Dispase (Gibco) in Ham's F10 (Gibco/Invitrogen) to liberate myofiber-associated cells.Cells of interest were sorted using a Becton-Dickenson FACSVantage flow cytometer with the FACSDiva option and FACSDiva software utilizing the immunophenotype Sca1- CD45-Ter119-Mac1-α7 Integrin+. Antibodies used are Ter-119 (eBioscience), CD45 (eBioscience), a-Mac1(eBioscience), Sca1(eBioscience), α7-Integrin(R&D Systems).

Protein extraction and immunoblotting

Cells were lysed by NP40 buffer (25 mM Hepes, 100 mM NaCl, 5 mM MgCl2, 10% glycerol, 0.2% NP-40, phosphatase inhibitor cocktail-1 and -2 (Sigma) and protease inhibitor cocktail (Roche).) for total proteins. When nuclear extraction is required, cells were extracted by CHEMICON Nuclear Extraction Kit (Millipore, #2900). Equal amounts of cell lysate were resolved by SDS-PAGE, transferred to polyvinylidene difluoride membranes (Millipore) and detected using an enhanced chemiluminescence system (Pierce Biotechnology). Primary antibodies used are HMGA2 (Cell Signaling, #5269) , α-Tubulin (Sigma, #T9026), IGF2BP2 (Abnova, #H00010644-M01), c-Myc (Cell Signaling, #9402), Sp1 (Abcam, # ab77441), IGF1R (Cell Signaling, # 9750).

Isolation of RNA and RT-PCR

Total RNAs were isolated by RNeasy Kits (Qiagen) and cDNA were made using iScript cDNA Synthesis Kit. SYBR Green dye based Quantitative Real Time PCR (qRT-PCR) was performed using SYBR Green PCR Master Mix and 7900HT Fast Real-Time PCR System from Applied Biosystems. Individual gene primers were designed and synthesized by Integrated DNA Technologies.

Muscle cross section area (CSA) analysis

Images of the entire Laminin stained tissue section were acquired using Scanscope (Aperio, Vista, California, USA) and the cross-sectional area of the individual fibers in the section measured automatically using a custom software, Astoria v3.0, developed at Novartis Institutes for Biomedical Research. Over 1,500 fibers in each section were measured automatically by this method. The mean ± standard error of the cross-sectional areas of the fibers in each muscle section was determined and the frequency distribution of fiber cross-sectional area plotted.